

Electronic Thesis and Dissertation Repository

8-13-2019 10:30 AM

Functional Magnetic Resonance Spectroscopy in First-Episode Schizophrenia: Measuring Glutamate and Glutathione Dynamics at 7-Tesla

Peter Jeon, *The University of Western Ontario*

Supervisor: Theberge, Jean, *The University of Western Ontario*

Joint Supervisor: Palaniyappan, Lena, *The University of Western Ontario*

A thesis submitted in partial fulfillment of the requirements for the Master of Science degree in Medical Biophysics

© Peter Jeon 2019

Follow this and additional works at: <https://ir.lib.uwo.ca/etd>



Part of the [Medical Biophysics Commons](#)

Recommended Citation

Jeon, Peter, "Functional Magnetic Resonance Spectroscopy in First-Episode Schizophrenia: Measuring Glutamate and Glutathione Dynamics at 7-Tesla" (2019). *Electronic Thesis and Dissertation Repository*. 6417.

<https://ir.lib.uwo.ca/etd/6417>

This Dissertation/Thesis is brought to you for free and open access by Scholarship@Western. It has been accepted for inclusion in Electronic Thesis and Dissertation Repository by an authorized administrator of Scholarship@Western. For more information, please contact wlsadmin@uwo.ca.

Abstract

Schizophrenia is a neuropsychiatric illness without known etiology or cure. Current efforts for symptom treatment still seem to leave a large portion of affected individuals without proper symptom management, with those experiencing symptom relief still having to wrestle with potential side-effects from medication trials. There has been growing evidence suggesting that glutamate and glutathione abnormalities hold major roles in development and manifestation of schizophrenia symptoms.

Magnetic resonance spectroscopy (MRS) provides a non-invasive means to observe *in-vivo* brain chemistry, including glutamate and glutathione. By adding a functional component to an MRS paradigm (fMRS), such as the color-word Stroop task, it is possible to detect potential changes in brain metabolite levels in response to a cognitive stimulus.

The objectives of this thesis were to determine whether a conventional short echo-time or longer echo-time semi-LASER sequence would be more suitable for measurements of an fMRS paradigm at 7.0-Tesla, and to apply this finding to the study of a group of never-medicated, first-episode schizophrenia (FES) individuals to track any potential abnormal glutamate and glutathione dynamics.

Contrary to previous beliefs that the shortest achievable echo-time would produce the most measurement signal, results from this study found that a long echo time (TE=100ms) produced very similar quality of measurements, with further benefits of long echo time being the removal of any macromolecular signal contribution.

Comparison of healthy controls (n = 25) to a FES population (n = 21) revealed no significant difference in resting or dynamic glutamate levels. However, resting and dynamic glutathione level were significantly different, suggesting potential glutathione regulation abnormalities, and, in extension, although not observed in this study, potential glutamate and glutamine abnormalities.

Future fMRS studies should investigate glutamate and glutathione dynamics from longitudinal data of FES follow-ups as well as between specific sub-groups within FES.

Keywords

Functional Magnetic Resonance Spectroscopy (fMRS), Schizophrenia, First-Episode Schizophrenia, Glutamate, Glutathione, Magnetic Resonance Imaging (MRI), 7.0-Tesla, Echo-Time (TE)

Summary for Lay Audience

Schizophrenia is an illness that affects the human brain and mind. Patients often hear voices and hold delusional beliefs. They often lack motivation and have trouble with attention and memory. Currently, there is no known cure or clear knowledge of its cause(s). Symptom treatment typically involves administering medication that regulates a brain chemical called dopamine. However, a large portion of patients do not respond to these medications, and after a few unsuccessful trials, this subgroup, declared non-responders, will be given Clozapine, which indirectly acts on another brain chemical called glutamate. Because of its side effects, Clozapine is left as a last resort. For non-responders, finding their way to an effective medication can be long and costly, usually leading to prolonged patient suffering and disability.

Measurements of brain chemicals glutamate and glutathione early in the illness have been shown, at resting levels, to potentially distinguish responders from non-responders. However, these measurements had not taken into account that brain glutamate levels change depending on the amount of brain activity, and so, we used functional magnetic resonance spectroscopy (fMRS) to measure changes of glutamate and glutathione levels in the brain during the performance of a task, the same specific brain activity for all participants. We believe these measurements will improve our ability to identify non-responders even before treatment begins.

This work shows that never medicated, first-episode patients with schizophrenia did not change glutamate levels significantly during the task, but did change glutathione levels differently compared to a cohort of healthy control individuals, which gives us hints about the chemicals involved in task difficulties and how to possibly treat them.

We hope that future work descending from these results will help psychiatrists develop ways to identifying non-responders upon first admission, and choose the right medication without delay.

Co-Authorship Statement

The following thesis contains work that will be submitted for publication with several co-authors. I (Peter Jeon) was responsible for recruiting a few of the healthy control volunteers for scanning as well as all data acquisition, post-processing, fitting, statistical analysis, and manuscript writing. Michael MacKinley was responsible for all other patient and healthy control volunteer recruitment as well as running cognitive tests. Kara Dempster was the acting clinical psychiatrist present for all patient scans who also made consensus diagnosis for all participants (alongside Dr. Lena Palaniyappan) using the Structured Clinical Interview for DSM-5. Dickson Wong developed the computer software used for data analysis. Drs. Jean Théberge and Lena Palaniyappan secured funding for this work, provided edits to the manuscript writing, devised the study plan, and supervised the research project.

Acknowledgments

To my supervisors, Dr. Jean Théberge and Dr. Lena Palaniyappan, thank you from the bottom of my heart for your continual patience and support toward my growth as a scientist. Having the two of you as my supervisors not only helped me as a graduate student, but also shaped me as a person in more ways than you might know. Dr. Théberge, you've challenged me to view my research as an honest exploration without compromise, and one I can really enjoy. Dr. Palaniyappan, your excitement and advice for me to develop an ongoing curiosity in my research pushes me even today to break past the boundaries of my knowledge and comfort. Many days, I wonder if both of you regret taking me on under your training, but I hope to reciprocate your kindness in the future years to come.

To my advisory committee members, Dr. Rob Bartha and Joe Gati, your genuine curiosity and seriousness toward my project has left a lasting impression of how much more ownership I should take of my research. Thank you.

To my research family, Michael MacKinley and Kara Dempster, I couldn't have asked for better coworkers. Thank you for making each meeting and scan session so interesting and enjoyable. To Trevor Szekeres and Scott Charlton, you guys make operating the 7T look like an art. Thank you for all your help and especially calming subjects during scan! To Dickson Wong, I don't know how I would have managed my projects without your expertise, help, and sacrifice. Your selflessness in research is something I strive to emulate as much as I can. Thank you. To Maria Densmore, how wonderful it was to have our offices so close to each other! Thank you for all the talks we had and for always making sure I was doing okay.

To my wife, Jumin, thank you for bearing with all my stress filled days and for giving me the opportunity to continue my studies. I am excited to go through this next season of my studies and life with you. To my parents, thank you for being the prime example of humility and patience in life and for your never-ending support toward my academic journey. I'm not quite there yet, but we will get there!

Lastly, I must acknowledge God whom I believe made everything possible. Thank You for reminding me that though I am not perfect, I have hope moving forward because of You.

Table of Contents

Abstract.....	ii
Summary for Lay Audience.....	iv
Co-Authorship Statement.....	v
Acknowledgments.....	vi
Table of Contents.....	vii
List of Tables.....	x
List of Figures.....	xi
List of Symbols and Abbreviations.....	xiii
List of Appendices.....	xv
Chapter 1.....	1
1 Introduction.....	1
1.1 Schizophrenia.....	1
1.1.1 Illness and Symptoms.....	1
1.1.2 Diagnosis and Treatment.....	2
1.1.3 Glutamate and Glutathione.....	3
1.2 Neuroimaging.....	4
1.2.1 Nuclear Magnetic Resonance (NMR).....	5
1.2.2 Magnetic Resonance Spectroscopy (MRS).....	8
1.2.3 Functional MRS (fMRS).....	9
1.3 Thesis Overview.....	11
1.4 References.....	13
Chapter 2.....	20
2 Observing metabolite changes in short versus long echo time functional magnetic resonance spectroscopy at 7-Tesla.....	20

2.1	Introduction.....	20
2.2	Methods.....	22
2.2.1	Participants.....	22
2.2.2	Functional Magnetic Resonance Spectroscopy	23
2.2.3	Cognitive Stimulus: Color-Word Stroop Task	24
2.2.4	Spectral Post-Processing.....	25
2.2.5	Statistical Analysis.....	26
2.3	Results.....	27
2.3.1	Spectral Fit, Quality, and Quantification	27
2.3.2	Metabolite Concentration.....	31
2.3.3	Metabolite Percentage Changes	34
2.3.4	Metabolite Correlation	36
2.4	Discussion.....	37
2.5	Conclusion	40
2.6	References.....	41
	Chapter 3.....	45
3	Dynamic glutamate and glutathione measurements in first-episode schizophrenia using 7-Tesla.....	45
3.1	Introduction.....	45
3.2	Methods.....	48
3.2.1	Participants.....	48
3.2.2	Functional Magnetic Resonance Spectroscopy	49
3.2.3	Cognitive Stimulus: Color-Word Stroop Task	50
3.2.4	Spectral Post-Processing.....	51
3.2.5	Statistical Analysis.....	52
3.3	Results.....	53

3.3.1	Stroop Task	53
3.3.2	Spectral Quality and Fit	54
3.3.3	Metabolite Concentration.....	58
3.3.4	Metabolite Dynamics	60
3.3.5	Correlation Analysis	62
3.4	Discussion	63
3.4.1	Glutamate and Glutathione Concentration.....	63
3.4.2	Dynamic Changes in Glutamate and Glutathione.....	64
3.4.3	Correlation	65
3.4.4	Limitations and Future Work.....	66
3.5	Conclusion	67
3.6	References	68
Chapter 4	73
4	Conclusion	73
4.1	Limitations	73
4.2	Future Works	74
4.3	References.....	76
Appendix A: Ethics Approval.....		77
Appendix B: Supplementary Figures.....		78
Curriculum Vitae		81

List of Tables

Table 2-1 Signal-to-noise ratio (SNR_{NAA}) and linewidth (LW_W) of spectra	30
Table 2-2 Coefficient of variation for each block of fMRS paradigm	30
Table 2-3 Cramer-Rao lower bound (CRLB) of each metabolite.....	31
Table 2-4 Pairwise comparison of glutamate and glutathione concentrations for adjacent blocks	32
Table 3-1 Summary of Stroop task performance	53
Table 3-2 Signal-to-noise ratio (SNR_{NAA}) and linewidth (LW_W).....	56
Table 3-3 Summary of coefficients of variation (CV).....	57
Table 3-4 Cramer-Rao lower bound (CRLB) values	57
Table 3-5 Pairwise comparison of glutamate and glutathione concentrations	58

List of Figures

Figure 1-1 Effect of external magnetic field on nuclei	6
Figure 1-2 Spin energy states.....	7
Figure 1-3 Example of resting MRS spectra and metabolites of interest	10
Figure 1-4 Example of fMRS time course.....	11
Figure 1-5 Illustration of expected metabolite abnormalities	12
Figure 2-1 Voxel position	27
Figure 2-2 Fit components of a human brain spectrum at TE=60ms	28
Figure 2-3 Fit components of a human brain spectrum at TE=100ms	29
Figure 2-4 Glutamate concentration estimates	33
Figure 2-5 Glutathione concentration estimates	34
Figure 2-6 Dynamic glutamate concentration changes.....	35
Figure 2-7 Dynamic glutathione concentration changes	36
Figure 2-8 Glutamate-glutathione concentration correlation.....	37
Figure 3-1 Voxel position	54
Figure 3-2 Spectral fit with metabolite components.....	55
Figure 3-3 fMRS glutamate concentration time-course.....	59
Figure 3-4 fMRS glutathione concentration time-course	60
Figure 3-5 fMRS glutamate dynamics	61
Figure 3-6 fMRS glutathione dynamics.....	62

Figure 3-7 Correlation of glutamate and glutathione concentrations 63

List of Symbols and Abbreviations

^1H	Proton
Δ	Change in
γ	Gyromagnetic ratio
ω_0	Larmor frequency
B_0	Externally applied static magnetic field
B_1	Magnetic field from radiofrequency coil
ACC	Anterior cingulate cortex
Ala	Alanine
Asp	Aspartate
Cho	Choline
Cr	Creatine
CSF	Cerebral spinal fluid
CV	Coefficient of Variation
ECC	Eddy current correction
fMRS	Functional magnetic resonance spectroscopy
GABA	Gamma-Aminobutyric Acid
Glc	Glucose
Gln	Glutamine
Glu	Glutamate
Gly	Glycine
GM	Grey matter
GSH	Glutathione
HSVD	Hankel singular value decomposition
Lac	Lactate
LASER	Localized by adiabatic selective refocusing
mM	milli-molar (mmol/L)
MR	Magnetic resonance
MRI	Magnetic resonance imaging
MRS	Magnetic resonance spectroscopy

Myo	Myo-inositol
NAA	<i>N</i> -acetyl aspartate
NAAG	<i>N</i> -acetyl aspartyl glutamate
NMDA	<i>N</i> -methyl- <i>D</i> -aspartate
Peth	Phosphorylethanolamine
ppm	Parts-per-million
PRESS	Point-resolved spectroscopy
RF	Radiofrequency
rmANOVA	Repeated measures analysis of variance
QUALITY	Quantification improvement by converting lineshapes to the Lorentzian type
QUECC	Combined QUALITY deconvolution and ECC
semi-LASER	Semi-localization by selective refocusing
SNR	Signal-to-noise ratio
Scyllo	Scyllo-inositol
STEAM	Stimulated echo acquisition mode
T ₁	Longitudinal relaxation time
T ₂	Transverse relaxation time
Tau	Taurine
TE	Echo Time
TI	Inversion Time
TR	Repetition Time
VAPOR	Variable pulse power and optimized relaxation delays
WM	White matter

List of Appendices

Appendix A Ethics approval.....	77
Appendix B Supplementary tables and figures.....	80

Chapter 1

1 Introduction

This thesis contains work that investigates neuroimaging in mental illness, specifically schizophrenia. Mental illnesses are those that affect an individual's mood, thinking, or behavior and can be a major concern when symptoms and stress start affecting a person's ability to function in everyday life. Schizophrenia is a complex disorder that affects around 1% of the population in Canada and worldwide^{1,2} and though the experience of the illness can vary from individual to individual, there is a potential for serious decline in quality of life if left untreated³⁻⁵. Currently, there is no known cure for schizophrenia as the exact causes and mechanisms of the illness are largely unknown. Hence, symptom management through various treatments remains the best hope for individuals with this illness. Early intervention in schizophrenia has been shown to greatly improve symptom treatment outcomes in individuals with hope of returning to normal functioning and lifestyles in society^{6,7}. While many illnesses and disorders are studied using definitive anatomical and physiological abnormalities to explain the causes of observed symptoms⁸⁻¹³, the lack of strong anatomical or physiological basis to fully explain the etiology of schizophrenia steered schizophrenia research to focus on potential mechanisms responsible for the symptoms observed in hopes that finding these chemical pathways will grant understanding as to which parts of the brain and in what form of brain abnormalities would cause the illness of schizophrenia¹⁴⁻¹⁶.

1.1 Schizophrenia

1.1.1 Illness and Symptoms

Schizophrenia is an illness of the mind and brain, affecting an individual's thoughts, emotions, and behavior. The illness is believed to have both genetic and environmental contributions¹⁶, including neurodevelopmental contributions where complications in early brain development remain dormant until symptoms typically start manifesting in the late teens to early twenties of an individual's life¹⁷. Though the exact cause of schizophrenia

is unknown, research has shown that certain factors increase the risk of illness development including having close family members with schizophrenia^{17,18}, experiencing complications at time of birth¹⁸⁻²⁰, experiencing social stress^{21,22}, and using cannabis early in youth^{23,24}.

Schizophrenia is characterized by a complex combination of positive, negative, and cognitive symptoms²⁵⁻²⁷. Positive symptoms refer to characteristics in individuals that appear added or distorted in reference to a healthy control population such as having hallucinations or delusions. Negative symptoms describe characteristics that seem reduced or lost and include traits such as social withdrawal, lack of emotions, or reduced motivation in everyday life. Lastly, cognitive symptoms describe any difficulties with attention, concentration, or memory and include having disorganized speech or thought. Not everyone with schizophrenia will experience the same combination of symptoms though certain symptoms have been shown to cluster together more than others²⁵.

Schizophrenia should be considered a major social issue because the social stigmas arising from a lack of public knowledge about those affected can not only be debilitating and demoralizing to patients and their families, but can also reduce access to care for other conditions that may be present²⁸. Furthermore, experiencing symptoms that distort one's functional and social abilities can lead to hardships in societal integration²⁹ as well as affect an individual's enjoyment to a quality of life that would otherwise be granted if not for their illness³⁰. Since some symptoms of schizophrenia fall into danger of potentially being easily dismissed erroneously, such as thinking that a child is simply lazy or introverted instead of seeing them as warning signs for schizophrenia development, it is important to establish reliable markers for early detection and proper diagnosis in schizophrenia so that appropriate care and treatment may be provided.

1.1.2 Diagnosis and Treatment

Diagnosis of schizophrenia usually involves multiple tests and screening along with certain criteria having to be met before full diagnosis of schizophrenia can be made.

Healthcare providers will look to rule out brain tumors, substance abuse, or other psychiatric disorders, such as bipolar disorder or major depressive disorder. According to the fifth edition of Diagnostic and Statistical Manual of Mental Disorders (DSM-5)³¹, if two or more of the following symptoms persist over a period of six months, a diagnosis of schizophrenia is appropriate: delusions, hallucinations, disorganized speech or catatonic behavior, negative symptoms, occupational or social dysfunction. After a trained physician completes the appropriate screenings and psychiatric evaluations, diagnostic criteria for schizophrenia can be made.

Currently, the first-line treatment for individuals with schizophrenia involves administration of antipsychotic medication that act on the dopamine pathways in the brain³². Though some individuals require additional medication trials using different antipsychotic medications, this first-line treatment generally helps to relieve and manage the positive symptoms of schizophrenia³². However, around 30% of individuals who receive this care will not respond to the antipsychotic medication and will have persisting positive symptoms along with negative and cognitive symptoms³³⁻³⁶. If treatment remains ineffective even after two additional antipsychotic medication trials, a drug called clozapine is usually suggested. Clozapine is often highly effective in reducing schizophrenia symptoms but is usually the last-line treatment due to its adverse side effects, one serious effect being a decrease in white blood cell count and an increase in risk for infection³³. Studies have suggested that clozapine can affect glutamate regulation in the brain and is perhaps why its administration shows different treatment responses than other dopamine-based antipsychotics in the 30% of treatment-resistant individuals³⁷⁻⁴⁰.

1.1.3 Glutamate and Glutathione

Glutamate is the human brain's most abundant excitatory neurotransmitter and has been hypothesized to play a role in symptoms observed in schizophrenia⁴¹⁻⁴³. Drugs such as ketamine and phencyclidine (PCP), when administered in subanesthetic doses, have produced a full range of positive, negative, and cognitive symptoms of schizophrenia⁴⁴.

Ketamine and PCP are known N-methyl-D-aspartate (NMDA) glutamate receptor antagonists^{44,45} giving rise to the glutamate NMDA hypofunction hypothesis of schizophrenia, or glutamate hypothesis of schizophrenia, which states that interference or blockage to the NMDA receptors promote glutamate release and possible excess⁴⁶. Having excess glutamate in the brain can lead to neurotoxicity and oxidative stress and without proper homeostatic regulations, could lead to neural dysfunction and death⁴⁷⁻⁴⁹.

Normally, glutathione (GSH) functions as the brain's first-line of defense against oxidative stress and works to protect any neuronal damage from free radicals. There is evidence to suggest that schizophrenia may be associated with the brain's inability to synthesize and regulate glutathione, without which, free radicals and glutamate excess would only keep increasing toxicity in the brain^{48,49}. Studies have also shown that glutathione depletion may lead to NMDA hypofunction⁴⁷⁻⁴⁹, suggesting that redox dysregulation and NMDA hypofunction in schizophrenia are tightly linked through a reciprocal relationship.

While resting measurements of glutamate and glutathione have revealed great insight as to potential physiological mechanisms behind schizophrenia symptoms, studying the dynamic regulations of these metabolites in individuals may provide another large piece of the puzzle toward understanding schizophrenia.

1.2 Neuroimaging

Many imaging modalities are available for the wide range of brain studies currently under investigation, each with their advantages and disadvantages. For the purposes of this thesis, magnetic resonance imaging (MRI) and spectroscopy (MRS) were chosen to investigate our research questions because of the following advantages: first, for a volunteer population that include individuals who experience psychosis or other symptoms triggered by stress or worry, MRI being free of ionizing radiation would encourage individuals to participate in our study as well as reduce worry of any potential side-effects from imaging. Secondly, MRI scanners are able to obtain a variety of

imaging information that allows for correlation and combination studies. This study was part of a larger study called TOPSY (Tracking Outcomes in Psychosis) where imaging sequences apart from anatomical imaging and spectroscopy were obtained from our volunteers to be used in the future (DTI and resting-state fMRI), but were not included for the purposes of this study. To understand the study design and tools used for this study, it is necessary to look into basic nuclear magnetic resonance (NMR) physics.

1.2.1 Nuclear Magnetic Resonance (NMR)

The first component of NMR to understand is that we are dealing with fundamental properties of atomic nuclei, more specifically, a fundamental property of particles within atoms (protons, neutrons, electrons), that we call nuclear spin angular momentum, S (Figure 1-1). A non-zero spin value in a nucleus will give rise to a magnetic moment, μ , of a nucleus, and can be expressed by,

$$\mu = \gamma \hbar S \quad \dots\dots (1)$$

where, γ is the gyromagnetic ratio and \hbar is the Planck's constant (h) divided by 2π . Atoms that possess an odd mass number or even mass number with odd number of protons and neutrons will have non-zero spin values. However, atoms with even mass number and even atomic number will possess zero spin with zero magnetic moment.

The next component of NMR involves the interaction of nuclear magnetic moments with an external magnetic field, B_0 (Figure 1-1). Quantum mechanics reveals that for a given spin, S , and magnetic field, B_0 , the Zeeman energy, E , which is the energy associated with the interaction between the magnetic moment and an external magnetic field, can be expressed as,

$$E = -\mu \cdot B_0 = -\gamma \hbar S \cdot B_0 \quad \dots\dots (2)$$

Furthermore, using the spin state quantum number, m_s , to represent values from $-S$, $-S+1$, ..., $+S$, all the different nuclear energy levels can be expressed by,

$$E = -\gamma\hbar m_s B_0 = \hbar\omega_0 m_s \quad \text{..... (3)}$$

where ω_0 , also known as the Larmor frequency, is equal to,

$$\omega_0 = -\gamma B_0 = 2\pi f_0 \quad \text{..... (4)}$$

For the purpose of this thesis, all further mentions of nucleus will refer to the hydrogen (^1H) nucleus, and by extension, a spin value of $S=1/2$. The Larmor frequency describes the rate of precession of a proton (for ^1H -NMR) about an external magnetic field and is directly proportional to the strength of B_0 . In the case of hydrogen nuclei, there are two energy states, lower energy and higher energy states. Since the Larmor frequency is dependent on B_0 , the energy difference based on Equation (3) of the two energy levels will also be dependent on the main magnetic field.

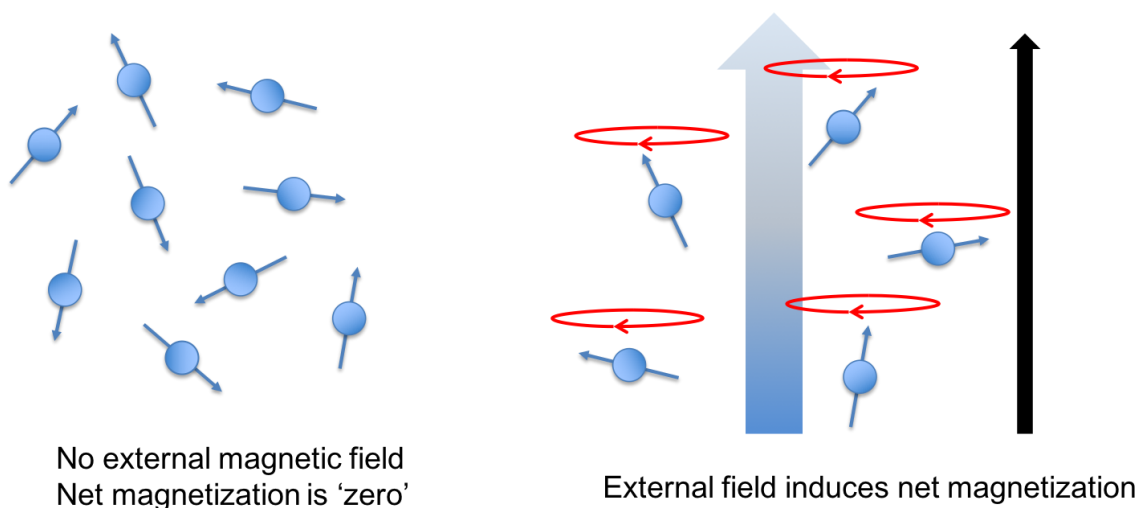


Figure 1-1 Effect of external magnetic field on nuclei

(left) For a sample of nuclei in thermal equilibrium, all nuclei will be in random orientation and will result in no net magnetization. *(right)* When an external magnetic field, B_0 , is introduced, the nuclei will begin precession around B_0 and induce a net bulk magnetization that can be measured.

The final component of NMR involves using resonance to induce spin state and energy level transitions. At the resonant frequency, nuclei are able to absorb energy to reach a higher energy state or dissipate energy to reach a lower energy state (Figure 1-2). In the presence of a static magnetic field in thermal equilibrium, the relative number of protons in each of the two energy states can be described by the Boltzmann distribution, which describes the balance between the tendency of spins to settle in the lower energy state and the pressure from thermal collision to produce random transitions between energy states, thereby equalizing the populations. In practice, there is a very small excess in the number of protons in the lower energy state ($\sim 23 \cdot 10^{-6}$ of total, at 7.0T), meaning that a large number of magnetic moments are necessary for detectable changes in bulk magnetization to be measured. This excess fraction of spins in the lower energy state is directly proportional to the main magnetic field strength, B_0 , with higher field strength helping more spins to remain in the lower energy state, and thereby playing a role in improved SNR at higher field strengths.

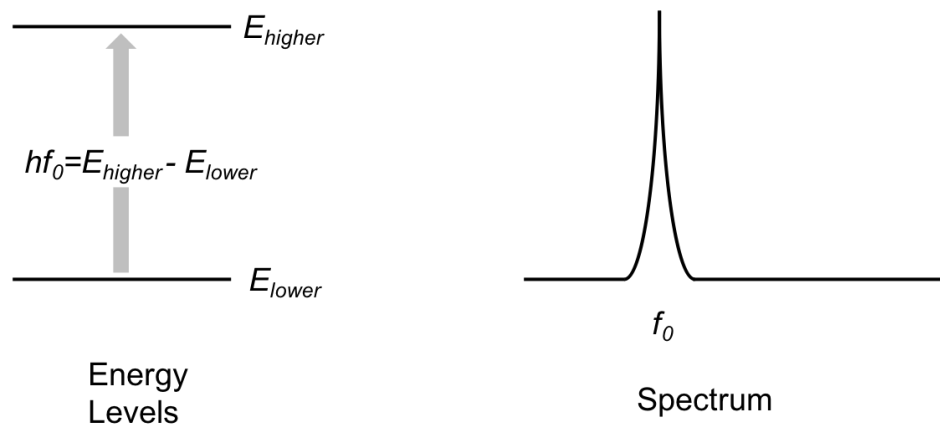


Figure 1-2 Spin energy states

(left) Nuclear energy levels are quantized and the difference in the two energy states will be associated with a specific frequency according to equation (3). *(right)* The frequency of each nuclei can then be represented in a spectrum of frequencies.

1.2.2 Magnetic Resonance Spectroscopy (MRS)

Using the properties of NMR, it is possible to use radiofrequency (RF) pulses to excite a specific volume, or voxel, of nuclei and attain a spectral signature of its contents. This technique is called magnetic resonance spectroscopy and it can be used to observe *in-vivo* human brain metabolites and their relative concentrations. MRI scanners are largely composed of the main magnet, which determines the main magnetic field strength, the gradient coils, which distorts the main magnetic field slightly in predictable ways, and the shim coils, which functions to adjust and improve field inhomogeneity. For voxel localization, RF pulses are applied with slice-selective gradients in three orthogonal planes. MRS signal will only be generated from the spins in the cubic (or rectangular prism) region of space formed by the intersection of these three planes.

In a homogenous B_0 , each nucleus will experience a slightly different total magnetic field due to the varying degree of shielding provided by the atom's electron cloud. This means that different molecular geometries, including bond lengths and bond angles, will contribute to the slight change of total magnetic field experienced by a particular nucleus, and by extension, its resonant frequency. This phenomenon is called chemical shift and helps distinguish nuclei from different molecules. Spectral signatures are often displayed in terms of chemical shift in units of ppm (parts-per-million) with peak intensity reflecting the relative number of equivalent ^1H within each molecule.

Since NMR detects frequency, the following equation is used to convert frequency in Hertz into chemical shift, δ , in ppm,

$$\delta(\text{ppm}) = 10^6 \cdot \frac{f - f_{ref}}{f_{ref}} \quad \dots\dots (5)$$

where f is the measured frequency of the nucleus under observation and f_{ref} is a reference frequency, usually DDS (4,4-dimethyl-4-silapentane-1-sulfonic acid), a compound widely used for spectroscopy calibrations due to its water-solubility and intense proton signal peak found much upfield than most organic molecular signals. The DDS peak is assigned a specific ppm value of 0. Another reference, especially in the human brain, is the NAA CH_3 peak, which is typically assigned a value of 2.01ppm. This is a useful way

of looking at spectra because different magnetic field strengths will yield different resonant frequencies according to equation 4 and so the distance between two nuclear peaks may appear different in one field strength as opposed to another. Using chemical shift ppm can eliminate magnetic field dependence in observation of singlet resonances and help to avoid confusion and facilitates consistency in spectral comparisons between various field strengths.

Several spectroscopy methods (or sequences) exist that are derivatives of using echoes of the free-induction-decay (FID) to make measurements. A few common sequences include PRESS (point-resolved spectroscopy), LASER (localized by adiabatic selective refocusing), semi-LASER, and STEAM (stimulated echo acquisition mode)⁵⁰. By using different RF pulse schema, these sequences provide different advantages as tools for spectroscopy measurement. For example, STEAM employs a 90° - 90° - 90° pulse scheme that allows for very short echo time acquisitions, hence allowing for less signal loss due to T_2 , T_2^* , and J-dephasing. PRESS (90° - 180° - 180°) and semi-LASER (90° - 180° - 180° - 180° - 180°) are spin-echo derived and have higher SNR per spectrum compared to STEAM (for a given echo time). This study will utilize the semi-LASER pulse sequence for its advantages over other sequences: 1) being more tolerant of B_1 inhomogeneity; 2) allowing a more precise excitation profile of the voxel (without unwanted signals from beyond the targeted voxel)⁵⁰. Other techniques such as the use of J-editing or quantum filtering were considered but not utilized because of sensitivity to motion, signal-to-noise ratio loss from subtraction methods, and general low signal yield^{51,52}.

1.2.3 Functional MRS (fMRS)

The mechanics of NMR and MRS can be taken further to study brain metabolite dynamics using functional MRS (fMRS) (Figure 1-3). As opposed to resting MRS which measures the molecular concentration levels during an assumed “resting state” (Figure 1-3), fMRS measures the molecular levels across a time course that includes a controlled resting baseline as well as a stimulus section (Figure 1-4). Various stimuli are available for an fMRS paradigm, such as visual⁵³⁻⁵⁵, cognitive task^{56,57}, or sensory pain stimuli^{58,59}.

Returning to our sample of individuals with schizophrenia, using a cognitive battery task during an fMRS paradigm may reveal any existing abnormal brain metabolite regulation.

An issue of resting MRS studies is that all spectra are averaged together regardless of the cognitive state of participants and without any instructions given regarding their cognitive state³⁷. Functional MRS deals with this issue by averaging by state and with instructions being given for both the rest and task states. Typical resting instructions would include gaze fixation and keeping the mind wandering without focusing on any particular topic for any length of time. Using this dynamic scale might be a more suitable marker for detecting and studying schizophrenia.

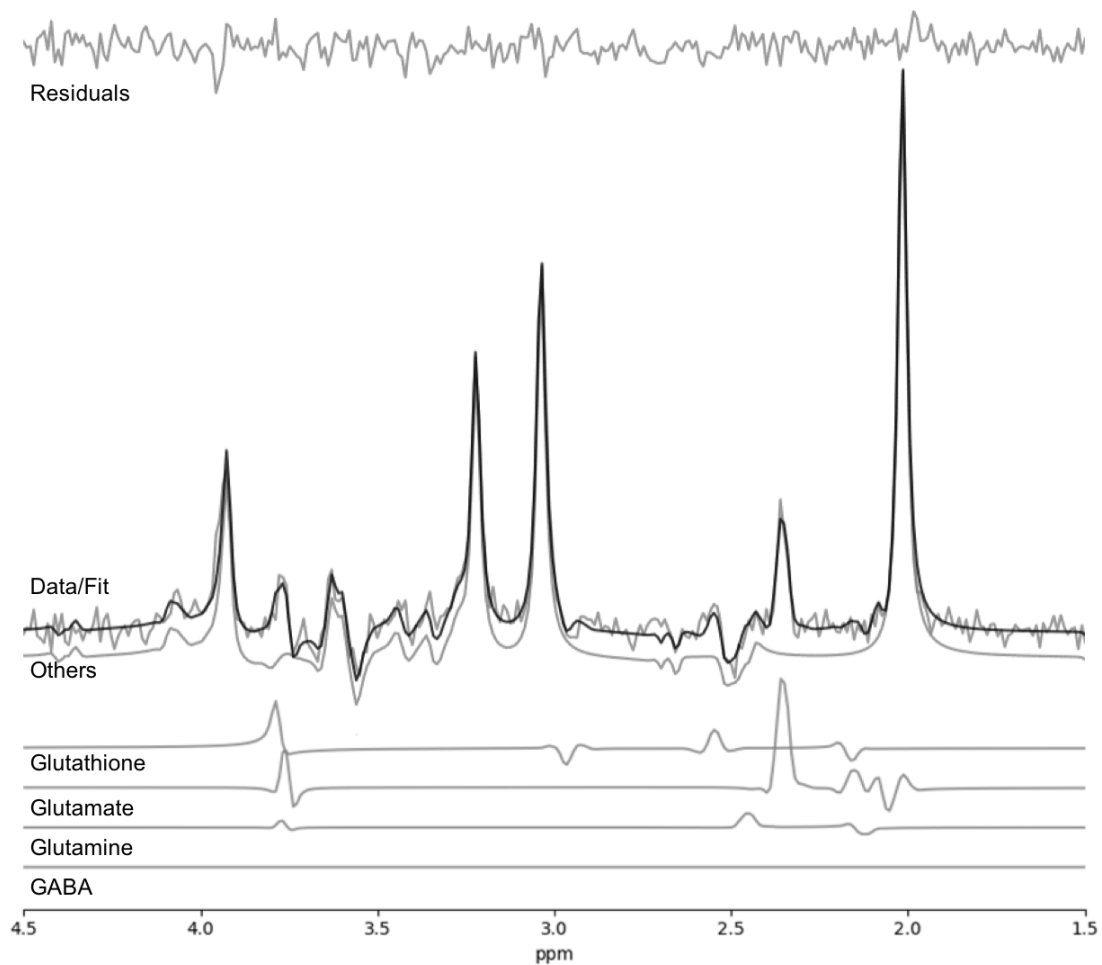


Figure 1-3 Example of resting MRS spectra and metabolites of interest

Illustration of spectral signatures of metabolites of interest. Spectrum was obtained using 7.0-Tesla MRS semi-LASER pulse sequence at TE=100ms. The sum of all individual metabolite spectral signatures produces the overall spectrum represented by ‘Data’ (light grey) line.

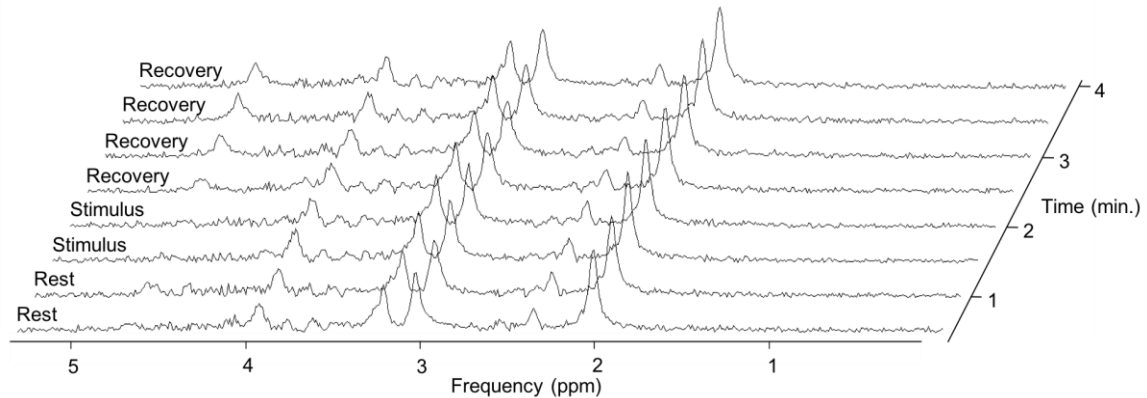


Figure 1-4 Example of fMRS time course

Sample illustration of an fMRS time course. As opposed to a single spectrum in static MRS, fMRS uses several spectra collected over a given time course, each representing part of a non-stimulus rest state or stimuli-introduced functional state.

1.3 Thesis Overview

The following two chapters of this thesis are works that look into the effects of glutamate and glutathione levels in individuals with first-episode schizophrenia. Chapter 2 is a methodological study investigating parameter optimization for functional magnetic resonance spectroscopy measurements at 7-Tesla. Chapter 3 is a direct application of the tools and methods established in the previous chapter to study glutamate and glutathione dynamics in a never-medicated first-episode schizophrenia population. The overall aim of this thesis is to study the dynamic glutamate and glutathione behaviors upon functional cognitive stimuli and recovery to baseline to better understand any potential glutamate

and glutathione regulation abnormalities in the brains of individuals with schizophrenia. Based on previous fMRS work in schizophrenia^{56,57}, we predict that the first-episode schizophrenia group will have elevated glutamate and lower glutathione levels compared to a healthy control population and that metabolite regulation abnormalities upon functional activation will be present in the form of delayed increases of lower amplitude in both metabolites (Figure 1-5). Once stimuli are removed, we expect to see a return to baseline in metabolite concentration levels.

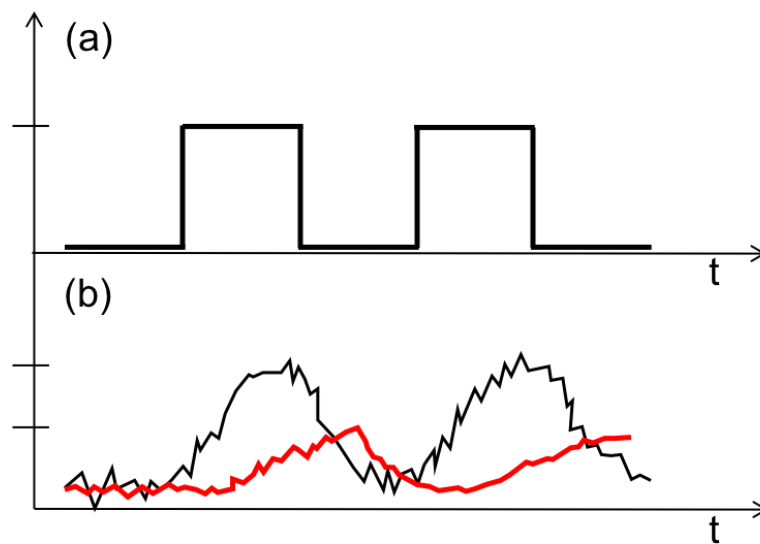


Figure 1-5 Illustration of expected metabolite abnormalities

Given a sample functional stimulus on/off pattern in (a), as was used in Taylor *et al.* 2015⁵⁶, we expect abnormalities in metabolite regulation (b) in the forms of (1) lower amplitude and (2) delayed response (indicated by the red line). The black line represents expected healthy metabolite behavior.

1.4 References

1. Saha S, Chant D, Welham J, Mcgrath J. A Systematic Review of the Prevalence of Schizophrenia. *PLoS Med.* 2005;2(5):413-433. doi:10.1371/journal.pmed.0020141
2. Moreno-Kustner B, Martin C, Pastor L. Prevalence of psychotic disorders and its association with methodological issues . A systematic review and meta-analyses. *PLoS One.* 2018;13(4):1-25.
3. Laursen TM, Nordentoft M, Mortensen PB. Excess Early Mortality in Schizophrenia. *Annu Rev Clin Psychol.* 2014;10:425-448. doi:10.1146/annurev-clinpsy-032813-153657
4. Olfson M, Gerhard T, Huang C, Crystal S, Stroup TS. Premature Mortality Among Adults With Schizophrenia in the United States. *JAMA Psychiatry.* 2015;72(12):1172-1181. doi:10.1001/jamapsychiatry.2015.1737
5. Simon GE, Stewart C, Yarborough BJ, et al. Mortality Rates After the First Diagnosis of Psychotic Disorder in Adolescents and Young Adults. *JAMA Psychiatry.* 2018;75(3):254-260. doi:10.1001/jamapsychiatry.2017.4437
6. Anderson KK, Norman R, Macdougall A, et al. Effectiveness of Early Psychosis Intervention : Comparison of Service Users and Nonusers in Population-Based Health Administrative Data. *Am J Psychiatry.* 2018;175:443-452. doi:10.1176/appi.ajp.2017.17050480
7. McGorry PD, Killackey E, Yung A. Early intervention in psychosis: concepts, evidence and future directions. *World Psychiatry.* 2008;7:148-156.
8. Rubinsztein DC. The roles of intracellular protein-degradation pathways in neurodegeneration. *Nature.* 2006;443:780-786.
9. Bredesen DE, Rao R V, Mehlen P. Cell death in the nervous system. *Nature.* 2006;443:796-802.

10. Liu Z, Zhou T, Ziegler AC, Dimitrion P, Zuo L. Oxidative Stress in Neurodegenerative Diseases: From Molecular Mechanisms to Clinical Applications. *Oxidative Med Cell Longevity*. 2017;2017:1-12.
11. Hashimoto M, Rockenstein E, Crews L, Masliah E. Role of Protein Aggregation in Mitochondrial Dysfunction and Neurodegeneration in Alzheimer's and Parkinson's Diseases. *NeuroMolecular Med*. 2003;4:21-35.
12. Vos KJ De, Grierson AJ, Ackerley S, Miller CCJ. Role of Axonal Transport in Neurodegenerative Diseases. *Annu Rev Neurosci*. 2008;31:151-173.
doi:10.1146/annurev.neuro.31.061307.090711
13. Sanchez AME, Mejia-Toiber J, Massieu L. Excitotoxic Neuronal Death and the Pathogenesis of Huntington's Disease. *Arch Med Res*. 2008;39:265-276.
doi:10.1016/j.arcmed.2007.11.011
14. Fornito A, Yucel M, Dean B, Wood SJ, Pantelis C. Anatomical Abnormalities of the Anterior Cingulate Cortex in Schizophrenia: Bridging the Gap Between Neuroimaging and Neuropathology. *Schizophr Bull*. 2009;35(5):973-993.
doi:10.1093/schbul/sbn025
15. Harrison PJ. Neuropathology of schizophrenia. *Psychiatry*. 2005;4(10):18-21.
16. Miyamoto S, Lamantia AS, Duncan GE, Sullivan P, Gilmore JH, Lieberman JA. Recent Advances in the Neurobiology of Schizophrenia. 2003;3(1):27-39.
17. Angermeyerl MC, Kiihn L. Gender Differences in Age at Onset of Schizophrenia. *Eur Arch Psychiatry Neurol Sci*. 1988;237:351-364.
18. Murray RM. Is schizophrenia a neurodevelopmental disorder? *Br Med J*. 1987;295(6600):681-682.
19. Rapoport JL, Addington AM, Frangou S, Psych MRC. The neurodevelopmental model of schizophrenia: update 2005. *Mol Psychiatry*. 2005;10:434-449.
doi:10.1038/sj.mp.4001642

20. Fatemi SH, Folsom TD. The Neurodevelopmental Hypothesis of Schizophrenia, Revisited. *Schizophr Bull.* 2009;35(3):528-548. doi:10.1093/schbul/sbn187
21. Corcoran BC, Walker E, Huot R, et al. The Stress Cascade and Schizophrenia: Etiology and Onset. *Schizophr Bull.* 2003;29(4):671-692.
22. Walker EF, Diforio D. Schizophrenia: A Neural Diathesis-Stress Model. *Psychol Rev.* 1997;104(4):667-685.
23. Henquet C, Murray R, Linszen D, Os J van. The Environment and Schizophrenia: The Role of Cannabis Use. *Schizophr Bull.* 2005;31(3):608-612. doi:10.1093/schbul/sbi027
24. Linszen DH, Dingemans PM, Lenior ME. Cannabis Abuse and the Course of Recent-Onset Schizophrenia Disorders. *Arch Gen Psychiatry.* 1994;51(4):273-279.
25. Kay SR, Sevy S. Pyramidal Model of Schizophrenia. *Schizophr Bull.* 1990;16(3):537-545.
26. Kay SR, Fiszbein A, A OL. The Positive and Negative Syndrome Scale (PANSS) for Schizophrenia. *Schizophr Bull.* 1987;13(2):261-276.
27. Liddle PF. The Symptoms of Chronic Schizophrenia: A Re-examination of the Positive-Negative Dichotomy. *Br J Psychiatry.* 1987;151:145-151.
28. Dickerson FB, Sommerville J, Origoni AE, Ringel NB, Parente F. Experiences of Stigma Among Outpatients With Schizophrenia. *Schizophr Bull.* 2002;28(1):143-155.
29. Hultman CM, Wieselgren I, Ohman A. Relationships between social support, social coping and life events in the relapse of schizophrenic patients. *Scand J Psychol.* 1997;38:3-13.
30. Drake RJ, Haley C, Akhtar S, Lewis SW. Causes and consequences of duration of

- untreated psychosis in schizophrenia. *Br J Psychiatry*. 2000;177(6):511-515.
31. First M, Williams J, Karg R, Spitzer R. Structured Clinical Interview for DSM-5 - Research Version (SCID-5 for DSM-5, Research Version; SCID-5-RV). *Am Psychiatr Assoc*. 2015.
 32. Murray RM, Lappin J, Forti M Di. Schizophrenia: From developmental deviance to dopamine dysregulation. *Eur Neuropsychopharmacol*. 2008;18:S129-S134. doi:10.1016/j.euroneuro.2008.04.002
 33. Agid O, Remington G, Kapur S, Arenovich T, Zipursky RB. Early Use of Clozapine for Poorly Responding First-Episode Psychosis. *J Clin Psychopharmacol*. 2007;27(4):369-373. doi:10.1097/jcp.0b013e3180d0a6d4
 34. Agid O, Schulze L, Arenovich T, et al. Antipsychotic response in first-episode schizophrenia: efficacy of high doses and switching. *Eur Neur*. 2013;23:1017-1022. doi:10.1016/j.euroneuro.2013.04.010
 35. Lally J, Ajnakina O, Forti M Di, et al. Two distinct patterns of treatment resistance: clinical predictors of treatment resistance in first-episode schizophrenia spectrum psychoses. *Psychol Med*. 2016;46:3231-3240. doi:10.1017/S0033291716002014
 36. Mouchlianitis E, Mccutcheon R, Howes OD. Brain imaging studies of treatment-resistant schizophrenia: a systematic review. *Lancet Psychiatry*. 2016;3(5):451-463. doi:10.1016/S2215-0366(15)00540-4.Brain
 37. Egerton A, Brugger S, Raffin M, et al. Anterior cingulate glutamate levels related to clinical status following treatment in first-episode schizophrenia. *Neuropsychopharmacology*. 2012;37(11):2515-2521. doi:10.1038/npp.2012.113
 38. Stone JM, Morrison PD, Pilowsky LS. Glutamate and dopamine dysregulation in schizophrenia – a synthesis and selective review. *J Psychopharmacol*. 2007;21(4):440-452.

39. Howes O, Mccutcheon R, Stone J. Glutamate and dopamine in schizophrenia: An update for the 21 st century. *J Psychopharmacol*. 2015;29(2):97-115. doi:10.1177/0269881114563634
40. Stone JM. Glutamatergic antipsychotic drugs: a new dawn in the treatment of schizophrenia? *Ther Adv Psychopharmacol*. 2011;1(1):5-18. doi:10.1177/2045125311400779
41. Coyle JT. Glutamate and Schizophrenia: Beyond the Dopamine Hypothesis. *Cell Mol Neurobiol*. 2006;26:365-384. doi:10.1007/s10571-006-9062-8
42. Moghaddam B, Javitt D. From revolution to evolution: the glutamate hypothesis of schizophrenia and its implication for treatment. *Neuropsychopharmacology*. 2012;37:4-15. doi:10.1038/npp.2011.181
43. Merritt K, Egerton A, Kempton MJ, Taylor MJ, Mcguire PK. Nature of Glutamate Alterations in Schizophrenia A Meta-analysis of Proton Magnetic Resonance Spectroscopy Studies. *JAMA Psychiatry*. 2016;73(7):665-674. doi:10.1001/jamapsychiatry.2016.0442
44. Javitt DC, Zukin SR. Recent advances in the phenciclidine model of schizophrenia. *Am J Psychiatry*. 1991;148(10):1301-1308. doi:10.1176/ajp.148.10.1301
45. Krystal JH, Karper LP, Seibyl JP, et al. Subanesthetic effects of the noncompetitive NMDA antagonist, ketamine, in humans. Psychotomimetic, perceptual, cognitive, and neuroendocrine responses. *Arch Gen Psychiatry*. 1994;51:199-214.
46. Coyle JT. NMDA receptor and schizophrenia: A brief history. *Schizophr Bull*. 2012;38(5):920-926. doi:10.1093/schbul/sbs076
47. Bitanirwe BKY, Woo TW. Oxidative stress in schizophrenia : An integrated approach. *Neurosci Biobehav Rev*. 2011;35:878-893. doi:10.1016/j.neubiorev.2010.10.008

48. Prabakaran S, Swatton JE, Ryan MM, et al. Mitochondrial dysfunction in schizophrenia: evidence for compromised brain metabolism and oxidative stress. *Mol Psychiatry*. 2004;9:684-697. doi:10.1038/sj.mp.4001511
49. Lin C, Lane H. Early Identification and Intervention of Schizophrenia: Insight From Hypotheses of Glutamate Dysfunction and Oxidative Stress. *Front Psychol*. 2019;10:1-9. doi:10.3389/fpsy.2019.00093
50. Scheenen TWJ, Klomp DWJ, Wijnen JP, Heerschap A. Short Echo Time 1 H-MRSI of the Human Brain at 3T With Minimal Chemical Shift Displacement Errors Using Adiabatic Refocusing Pulses. *Magn Reson Med*. 2008;59:1-6. doi:10.1002/mrm.21302
51. Near J, Evans CJ, Puts NA, Barker PB, Edden RA. J-difference editing of GABA: simulated and experimental multiplet patterns. *Magn Reson Med*. 2013;70(5):1-17. doi:10.1002/mrm.24572.J-difference
52. Claridge T. Correlations Through the Chemical Bond I: Homonuclear Shift Correlation. In: *High-Resolution NMR Techniques in Organic Chemistry*. 3rd ed. Oxford: Elsevier Science; 2016:203-241.
53. Mangia S, Tkáč I, Gruetter R, et al. Sensitivity of single-voxel 1H-MRS in investigating the metabolism of the activated human visual cortex at 7T. *Magn Reson Imaging*. 2006;24(4):343-348. doi:10.1016/j.mri.2005.12.023
54. Mangia S, Tka I, Gruetter R, Moortele P-F Van de, Maraviglia B, Ugurbil K. Sustained neuronal activation raises oxidative metabolism to a new steady-state level : evidence from 1 H NMR spectroscopy in the human visual cortex. *J Cereb Blood Flow Metab*. 2007;27:1055-1063. doi:10.1038/sj.jcbfm.9600401
55. Lin Y, Stephenson MC, Xin L, Napolitano A, Morris PG. Investigating the metabolic changes due to visual stimulation using functional proton magnetic resonance spectroscopy at 7T. *J Cereb Blood Flow Metab*. 2012;32:1484-1495. doi:10.1038/jcbfm.2012.33

56. Taylor R, Schaefer B, Densmore M, et al. Increased glutamate levels observed upon functional activation in the anterior cingulate cortex using the Stroop Task and functional spectroscopy. *Neuroreport*. 2015;26(3):107-112.
doi:10.1097/WNR.0000000000000309
57. Taylor R, Neufeld RWJ, Schaefer B, et al. Functional magnetic resonance spectroscopy of glutamate in schizophrenia and major depressive disorder: anterior cingulate activity during a color-word Stroop task. *npj Schizophr*. 2015;1:15028.
doi:10.1038/npj schz.2015.28
58. Mullins PG, Rowland TLM, Jung RE, Sibbitt WL. A novel technique to study the brain's response to pain: Proton magnetic resonance spectroscopy. *Neuroimage*. 2005;26:642-646. doi:10.1016/j.neuroimage.2005.02.001
59. Gussew A, Rzanny R, Erdtel M, et al. Time-resolved functional 1H MR spectroscopic detection of glutamate concentration changes in the brain during acute heat pain stimulation. *Neuroimage*. 2010;49:1895-1902.
doi:10.1016/j.neuroimage.2009.09.007

Chapter 2

2 Observing metabolite changes in short versus long echo time functional magnetic resonance spectroscopy at 7-Tesla

This work is a methodological study examining healthy control volunteers to determine the optimal functional magnetic resonance spectroscopy parameters to use for future clinical studies involving individuals with schizophrenia.

2.1 Introduction

Proton magnetic resonance spectroscopy ($^1\text{H-MRS}$) has been instrumental in clinical and research settings for observing *in-vivo* human molecular chemistry. Studies involving brain magnetic resonance imaging (MRI) and MRS have especially pushed the boundaries of how we can study the human brain and increase our understanding of brain mechanisms on a chemical level. This is important particularly for mental illnesses such as schizophrenia where the exact pathophysiological mechanisms responsible for symptoms remain in question.

Schizophrenia symptoms are largely categorized into positive, negative and cognitive symptoms and individuals with schizophrenia may experience any combination of these symptoms in varying degrees. Current first-line treatment methods include the administration of antipsychotics that act on the dopaminergic pathways of the brain and have been useful for managing the positive symptoms of schizophrenia in many patients¹. However, around a third of people with schizophrenia do not seem to get better with this first-line treatment suggesting an alternative or additional pathway responsible for the negative and cognitive symptoms experienced by these individuals²⁻⁵. One leading hypothesis is the N-methyl D-aspartate (NMDA) hypofunction hypothesis, which proposes that the NMDA glutamate receptors' reduced functioning is the cause of the symptoms of this illness. Previous findings that support this hypothesis involve administering subanesthetic doses of phencyclidine (PCP) and ketamine, both NMDA

receptor antagonists, to subjects to find that the full range of schizophrenia symptoms was replicated, including negative and cognitive symptoms^{6,7}.

Though postmortem studies have found similar results in the past, the rapid changes of proteins after death put constraints on how brain molecular chemistry can be studied. MRS offers a solution to such constraints, as we are now able to observe *in-vivo* human brain metabolites non-invasively without the use of any harmful ionizing radiation. Much attention has been drawn to studying glutamate in the human brain in hopes to prove glutamatergic contribution in the pathophysiology of the full range of schizophrenia symptoms⁸⁻¹². For example, elevated resting glutamate levels in individuals with schizophrenia may suggest NMDA receptor hypofunction as well as glutamate excitotoxicity due to excess^{13,14}. This has extended to studies of related metabolites such as glutathione (GSH), an important antioxidant in the human body, which may provide protection against oxidative stress in the brain^{15,16}. Conversely, inability to regulate GSH properly may make brain excitotoxicity worse, possibly linking the two metabolites to symptoms observed in non-responding patients with schizophrenia. Finding the mechanisms responsible for negative and cognitive symptoms could help distinguish those who are treatment responders to the first-line medication from those who are treatment-resistant to dopamine-based drugs. Since earlier treatment has been linked to better patient symptom outcome in schizophrenia, individuals falling in the treatment-resistant group would benefit from finding the right treatment plan earlier rather than suffering a prolonged period of time under an ineffective first-line treatment only to find later that they would have to find alternative treatment methods^{17,18}.

Previous work by Egerton *et al.* (2012)⁹ showed that abnormal resting glutamate levels were linked to poor treatment outcome in first-line treatments. However, since glutamate is the brain's main excitatory neurotransmitter, various brain activities are able to alter glutamate levels, especially if the resting state is not well controlled for. Because of this, dynamic glutamate measurements using functional MRS (fMRS) may be a more sensitive early marker in treatment outcome in schizophrenia. Functional MRS uses spectral acquisitions at specific time points to track changes in human brain metabolites in response to a functional stimulus. Any abnormalities in glutamate or GSH dynamics in

individuals with schizophrenia and within their symptom subgroups may reveal a clearer picture of the specific mechanisms responsible for the full range of schizophrenia symptoms.

Conventional MRS sequences use a short or “short-as-possible” echo time to minimize the T_2 relaxation and J-dephasing effects. However, a recent study by Wong *et al.* (2018)¹⁹ examined an array of echo times and identified an optimum TE value for *in vivo* glutamate measurement for the 7.0-Tesla semi-LASER sequence to be near TE = 105ms. This chapter presents a preliminary study to determine whether the conventional short echo time or the proposed longer echo time would be more appropriate in detecting the glutamate and GSH dynamics in an fMRS paradigm. We believe this tool is necessary to investigate in healthy individuals before introducing to a patient population. In this work, we implement an fMRS paradigm using the color-word Stroop task with one activation block and a recovery block that is twice the length of the activation block to observe metabolite recovery behaviors. We expect that both short and long echo times will show significant increases in glutamate and GSH upon functional activation and that both metabolite levels will return to baseline within the recovery period timeframe.

2.2 Methods

2.2.1 Participants

Twelve healthy control volunteers were recruited for this study who gave informed written consent according to the guidelines of the Human Research Ethics Board for Health Sciences at the University of Western Ontario (Appendix A). Though a patient population was not included in this particular work, all healthy controls were matched with our first-episode schizophrenia recruits for age, gender and parental socio-economic status in order to allow inclusion into the healthy cohort of Chapter 3. Screening was done on each participant for any significant head injury, major medical illness, or magnetic resonance imaging (MRI) contraindications.

2.2.2 Functional Magnetic Resonance Spectroscopy

All fMRS measurements were made at the Centre for Functional and Metabolic Mapping (CFMM) at the University of Western Ontario using a Siemens MAGNETOM 7-Tesla MRI scanner along with a head-only radiofrequency coil having 8 transmit channels and 32 receive channels. A two-dimensional turbo spin echo sequence obtained in the sagittal direction (37 slices, TR=8000ms, TE=70ms, flip-angle (α)=120°, thickness = 3.5mm, field of view = 240×191mm, echo-train length = 7) was used as reference to place a 2.0 x 2.0 x 2.0 cm (8cm³) ¹H-MRS voxel on the bilateral dorsal anterior cingulate cortex (dACC) where robust activation was observed based on previous work using the same color-word Stroop task^{20,21}.

One short (TE=60ms) and one long (TE=100ms) echo time was used for each scan session using the semi-LASER ¹H-MRS pulse sequence (TR=7500ms, bandwidth = 6000Hz, N = 2048). For the purpose of this study, descriptions of ‘short’ or ‘long’ echo times were chosen based on minimum echo time available and falling within the range of glutamate’s optimal echo times found by Wong *et al.* (2019)¹⁹, respectively^a. Using the shortest echo time aimed to maximize the signal by minimizing signal lost to T₂ relaxation while using the long echo time minimized glutamate signal loss due to J-dephasing of glutamate’s MNPQ multiplet and minimized macromolecular signal contributions. Localized B_0 and B_1 shimming, frequency and power calibrations were completed before each data set collection. For each echo time, 128 channel-combined spectral averages were acquired, each of which were water-suppressed using the VAPOR preparation sequence. A water-unsuppressed spectrum was also acquired to use as reference for spectral post-processing and quantification.

The fMRS paradigm of both echo times consisted of the same four-minute by four-block model. The first block, labeled ‘Rest’, measured resting metabolite levels. The second

^a It is understood that the expressions “short” and “long” used to describe echo times have different meanings in other contexts and that an echo time of 60ms could be considered long relative to the T₂ of human brain metabolites or extremely long in the context of NMR measurements in solids. Here, it is called short only in relation to the even longer optimal echo time for glutamate.

block, labeled ‘Stroop’, measured metabolite changes in response to functional activation by the color-word Stroop task. The third and fourth blocks were the ‘Recovery 1’ and ‘Recovery 2’ blocks to observe the recovery behaviors of metabolite levels after the cognitive stimulus was removed. The order of echo times for scanning was randomized into equal proportions with approximately one minute between each scan to allow set-up of sequence as well as letting participants know of the upcoming sequence. Volunteers were not taken out of the scanner during the entirety of the scan session and adjustments were not necessary between echo time changes.

2.2.3 Cognitive Stimulus: Color-Word Stroop Task

PsychoPY²² was used to implement a color-word Stroop task as the functional activation method for our fMRS paradigm. Volunteers were given a hand-held controller with four colored buttons (yellow, red, green, blue) to be used to respond to one of four categories of words they saw on a projected screen of 50% gray background within the MR scanner: congruent, incongruent, word-only, color-only. This protocol was chosen based on previous work by Taylor *et al.* (2015) that showed reliable activation of the anterior cingulate¹⁹. The instructions given to subjects were to respond, using the controller, to the color that they saw on the screen, regardless of what the actual word spelled out. The only condition where volunteers would press what the word actually spelled out would be the ‘word-only’ category in which no color (white text) would be presented with the text. Each word stimulus was presented for 2s followed by a cross fixation for 1s. This protocol lasted for four minutes during the ‘Stroop’ block of the fMRS paradigm. Each of the other four-minute blocks were simple cross fixations with instructions to keep the mind as blank as possible to simulate as close to a true resting state that could be observed during this protocol. To ensure that all participants understood and were able to perform the Stroop task, an 80% response accuracy threshold was required during a practice session held in a room near the MRI suite prior to starting the scanning session.

2.2.4 Spectral Post-Processing

For each echo time, the 128 frequency- and phase-corrected spectra were sequentially grouped by 32 spectra each, then averaged, to produce 4 final spectra representing each block of the fMRS paradigm²³. These 4 spectra underwent QUALITY Eddy Current Correction (QUECC)²⁴ post-processing, with 400 QUALITY (quantification improvement by converting lineshapes to the Lorentzian type) points, to reduce any linewidth distortions and the Hankel Singular Value Decomposition (HSVD) water removal to remove any residual water signal between 4.2ppm and 5.7ppm. Afterwards, each spectrum ran through fitMAN^{19,25}, a spectral fitting routine that uses echo time-specific templates, modelled with PyGAMMA²⁸, in a Levenberg-Marquardt iterative, non-linear minimization algorithm in the time domain.

Eighteen brain metabolites included in the fitting template were: alanine, aspartate, choline, creatine, γ -aminobutyric acid (GABA), glucose, glutamate, glutamine, glutathione, glycine, lactate, myo-inositol, N-acetyl aspartate, N-acetyl aspartyl glutamate, phosphorylethanolamine, scyllo-inositol, and taurine. Macromolecules were added in the fitting template for only TE=60ms using fourteen Lorentzian lineshapes constrained and fixed for relative amplitudes and linewidths between macromolecule resonances. A single phase parameter was used for all macromolecular resonances. The water unsuppressed spectrum was fit as well, using fitMAN, into a single peak for use during quantification calculations.

Metabolite concentrations were quantified using Barstool¹⁹ through voxel locations mapped onto 0.75mm isotropic T₁-weighted images collected using an MP2RAGE sequence (TR=6000ms, TI₁=800ms, TI₂=2700ms, flip-angle 1 (α_1)=4°, flip-angle 2 (α_2)=5°, FOV=350mm×263mm×350mm, T_{acq}=9min. 38secs, iPAT_{PE}=3 and 6/8 k-space), for each participant. Gray matter, white matter, and CSF tissue fractions in the voxel were calculated by partial volume segmentation to correct for tissue-specific T₁ and T₂ relaxations during quantification.

2.2.5 Statistical Analysis

Mean metabolite concentrations and standard deviations were calculated for glutamate and glutathione at both echo times. Paired heteroscedastic t-tests were used to compare means of each metabolite at short and long echo time. Four measures were used to compare the quality of signal and quantification between short and long echo time. First, signal-to-noise ratio (SNR_{NAA}) was calculated using the frequency domain amplitude of the NAA CH_3 peak of each spectrum and dividing it by the standard deviation of the noise in the last 32 points most upfield of the spectrum. Second, the linewidth, using full-width-at-half-max (FWHM), of the water-unsuppressed spectra was calculated. Third, Cramer-Rao lower bound values were computed using Barstool¹⁹. Lastly, group coefficient of variation was calculated by dividing the standard deviation of metabolite concentration from each individual of the group by the group's mean metabolite concentration.

To assess any differences in effect at the dynamic level, metabolite concentration percentage changes were calculated using

$$\% \Delta [\textit{metabolite}] = \frac{[\textit{metabolite}] - [\textit{metabolite}]_{\textit{baseline}}}{[\textit{metabolite}]_{\textit{baseline}}} \times 100\%,$$

where $[\textit{metabolite}]$ is the concentration of the metabolite at the time of interest during the Stroop paradigm and $[\textit{metabolite}]_{\textit{baseline}}$ is the concentration of the metabolite acquired from the first post-processed spectral average. Two-sample equal variance (homoscedastic) t-tests were used to calculate any significant differences in metabolite concentration percentage changes between the two echo times.

Lastly, to investigate the strength of co-occurrence between changes of the two metabolites, Pearson correlation analysis was performed between individual glutamate and glutathione concentrations across all four time-points of the fMRS paradigm (Rest, Stroop, Recovery 1, Recovery 2). All statistics were performed using SPSS²⁶.

2.3 Results

2.3.1 Spectral Fit, Quality, and Quantification

A sample voxel positioning in the bilateral dorsal ACC is shown in Figure 2-1. Figure 2-2 and Figure 2-3 show sample fittings of frequency and phase corrected spectra along with a detailed breakdown of metabolite components at TE=60ms and TE=100ms, respectively, both from the same volunteer.

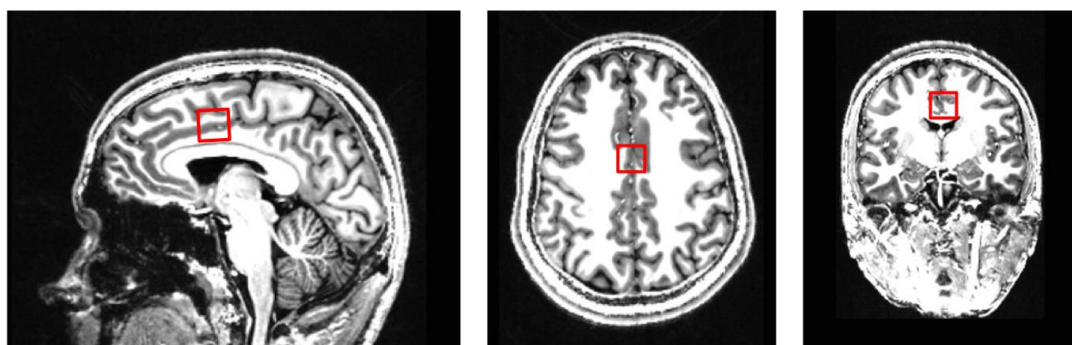


Figure 2-1 Voxel position

A 2cm x 2cm x 2cm voxel (*red*) placed in the dorsal anterior cingulate cortex (ACC) in the sagittal (*left*), transverse (*middle*), and coronal (*right*) view.

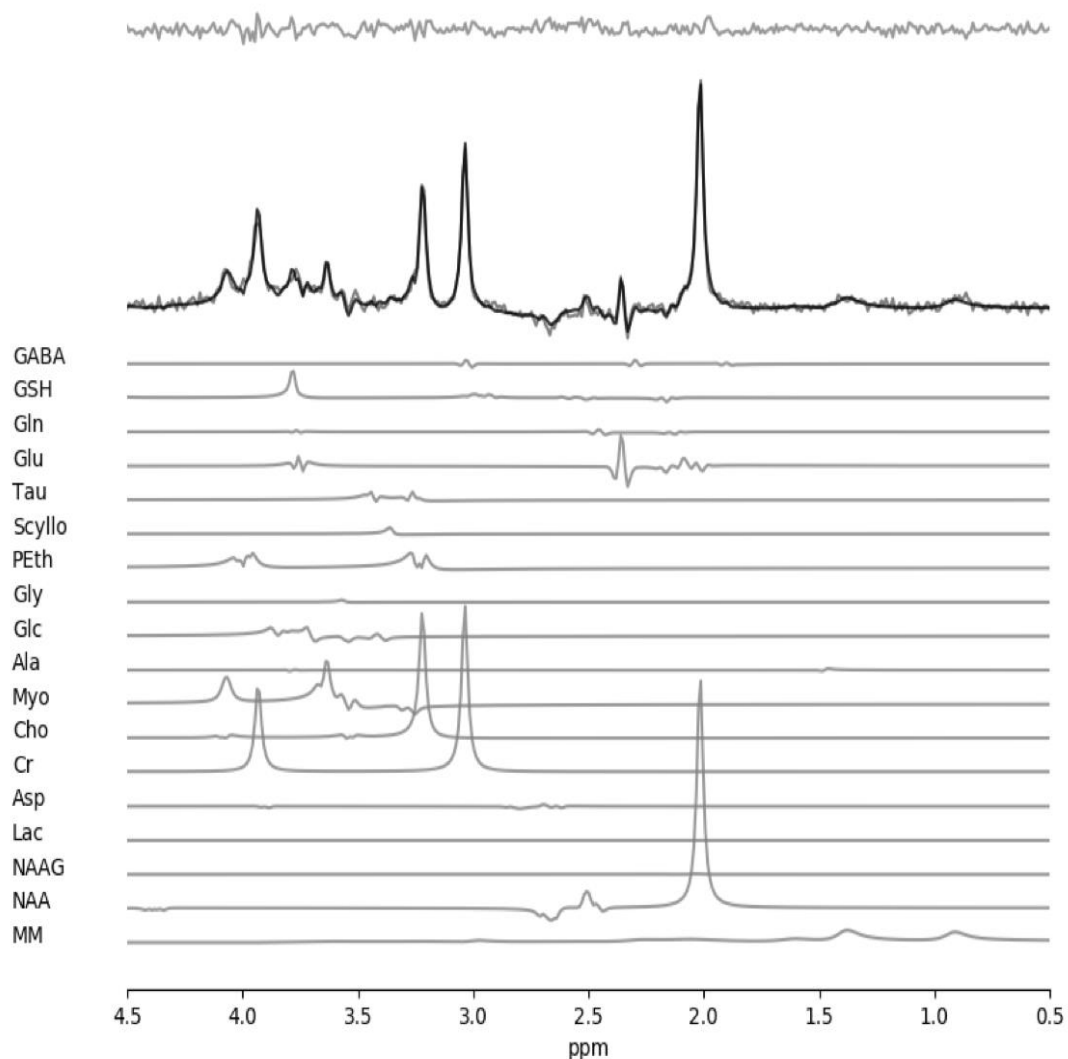


Figure 2-2 Fit components of a human brain spectrum at TE=60ms

The sum of individual metabolite spectral signatures produces the overall spectrum observed. The bolded black line represents the final fit spectrum overlaid on the raw data (light grey) from a participant of this study. Individual spectral components are shown below the fitted spectrum. A 1Hz exponential filter was applied for display only.

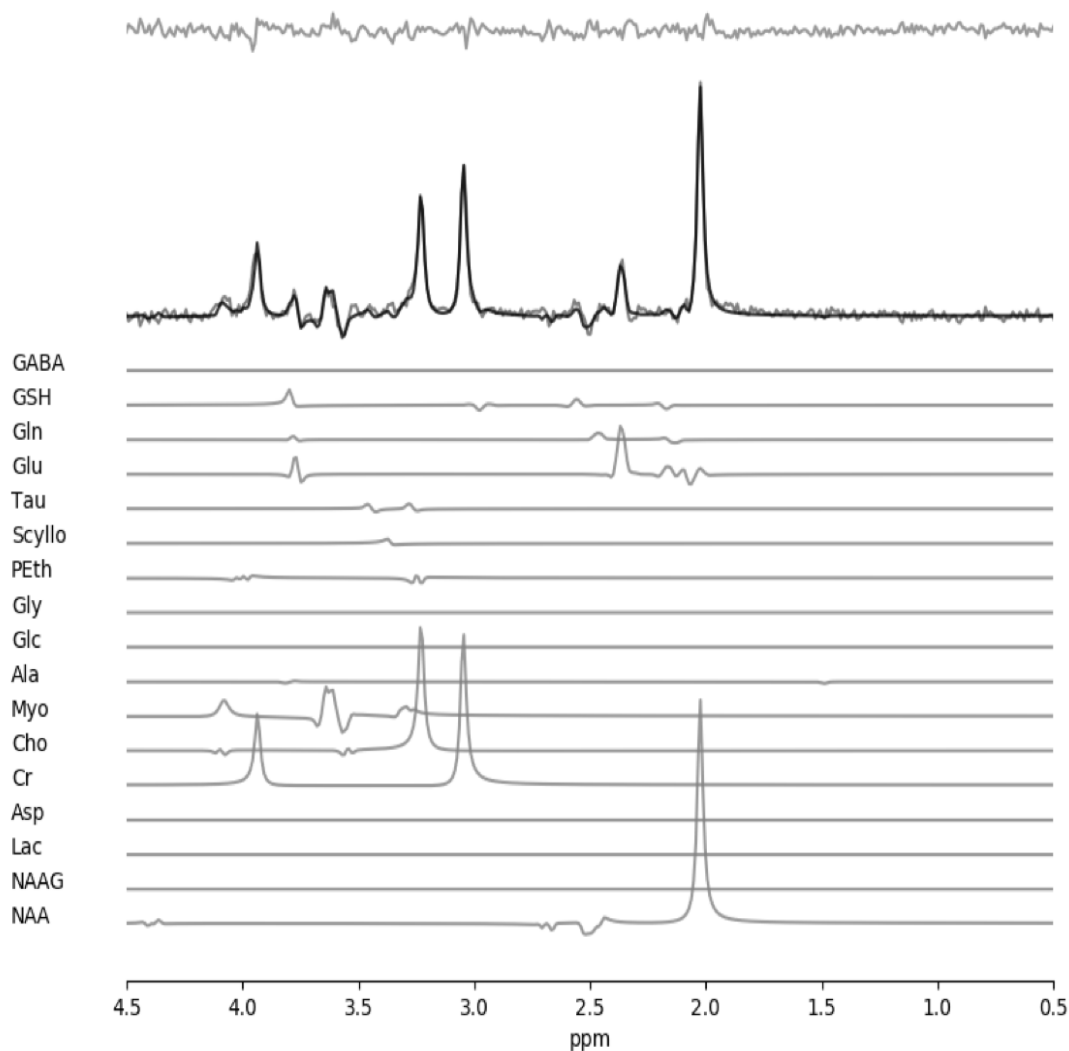


Figure 2-3 Fit components of a human brain spectrum at TE=100ms

The sum of individual metabolite spectral signatures produces the overall spectrum observed. The bolded black line represents the final fit spectrum overlaid on the raw data (light grey) from the same participant as Figure 2-2. Individual spectral components are shown below the fitted spectrum. A 1Hz exponential filter was applied for display only.

Four measures comparing spectral quality between TE=60ms and TE=100ms are highlighted in Tables 2-1, 2-2, and 2-3. The water linewidth (LW_w) revealed no

significant difference between TE=60ms (M=7.25, SD=1.14) and TE=100ms (M=6.92, SD=1.24); $t(22) = 0.686$, $p = 0.50$ (Table 2-1). Likewise, the coefficients of variation were not significantly different between the short and long echo times (Table 2-2). Cramer-Rao lower bound (CRLB) values were significantly lower for glutamate ($t(94) = 10.204$, $p < 0.001$) but significantly higher for glutathione ($t(94) = -8.443$, $p < 0.001$) at TE=100ms (M=3.24, SD=0.77; M=9.35, SD=2.00) compared to TE=60ms (M=6.06, SD=1.76; M=6.33, SD=1.47) (Table 2-3).

<i>Echo Time (TE)</i>	SNR_{NAA}	LW_W
<i>TE=60ms</i>	180±50	7.3±1.1 Hz
<i>TE=100ms</i>	225±42	6.9±1.2 Hz

Table 2-1 Signal-to-noise ratio (SNR_{NAA}) and linewidth (LW_W) of spectra

Mean SNR_{NAA} and LW_W (N=12) calculated from average of total fMRS data for TE=60ms and TE=100ms, with standard deviation.

<i>Group</i>	<i>Rest</i>	<i>Stroop</i>	<i>Recovery1</i>	<i>Recovery2</i>
<i>TE=60ms</i>				
[Glu]	16.3	16.8	15.1	14.3
[GSH]	14.4	17.9	15.4	12.3
<i>TE=100ms</i>				
[Glu]	16.6	16.9	19.5	17.8
[GSH]	16.7	12.7	16.8	16.0
<i>TE=60ms vs</i> <i>TE=100ms</i>				
[Glu]	$p = 0.95$ ($F = 1.04$)	$p = 0.99$ ($F = 1.01$)	$p = 0.42$ ($F = 1.65$)	$p = 0.49$ ($F = 1.53$)
[GSH]	$p = 0.64$ ($F = 1.34$)	$p = 0.28$ ($F = 0.51$)	$p = 0.78$ ($F = 1.19$)	$p = 0.40$ ($F = 1.67$)

Table 2-2 Coefficient of variation for each block of fMRS paradigm

Coefficient of variation (CV) expressed as a percentage for glutamate and glutathione at TE=60ms and TE=100ms. Comparison of CV between the two echo times are shown for each fMRS paradigm block.

<i>Group</i>	<i>CRLB (%)</i>
<i>TE=60ms</i>	
[Glu]	6.06±0.25
[GSH]	6.63±0.21
<i>TE=100ms</i>	
[Glu]	3.24±0.11
[GSH]	9.35±0.29

Table 2-3 Cramer-Rao lower bound (CRLB) of each metabolite

Mean CRLB, expressed as a percentage, for glutamate and glutathione concentration estimates at TE=60ms (N=12) and TE=100ms (N=12) across all fMRS blocks, with standard deviation.

2.3.2 Metabolite Concentration

Glutamate and glutathione concentrations, during short and long echo times, for the four blocks of the ¹H-fMRS paradigm are summarized in Table 2-4. Pairwise comparison of adjacent blocks revealed significant decrease in glutamate concentration ($t(11) = 4.138$, $p < 0.005$) from Recovery 1 ($M=6.64$, $SD=1.29$) to Recovery 2 ($M=6.35$, $SD=1.13$) at TE=100ms as well as significant decrease in glutathione concentration ($t(11) = 2.416$, $p < 0.05$) from Rest ($M=2.79$, $SD=0.40$) to Stroop ($M=2.64$, $SD=0.47$) for TE=60ms. A strong trend toward increasing glutamate levels ($t(11) = -2.012$, $p = 0.07$) was also observed between Stroop ($M=6.47$, $SD=1.10$) and Recovery 1 ($M=6.64$, $SD=1.29$) at TE=100ms.

<i>Group</i>	<i>p(Stroop- Rest)</i>	<i>p(Rec1- Stroop)</i>	<i>p(Rec1- Rec2)</i>	<i>Rest</i>	<i>Stroop</i>	<i>Recovery1</i>	<i>Recovery2</i>
<i>TE=60ms</i>							
[Glu]	0.431	0.185	0.653	9.31±0.44	9.53±0.46	9.25±0.40	9.34±0.38
[GSH]	0.034	0.326	0.503	2.79±0.12	2.64±0.14	2.73±0.12	2.77±0.10
<i>TE=100ms</i>							
[Glu]	0.460	0.069	0.002	6.52±0.31	6.47±0.32	6.64±0.37	6.35±0.33
[GSH]	0.181	0.660	0.832	1.51±0.07	1.61±0.06	1.64±0.08	1.63±0.08

Table 2-4 Pairwise comparison of glutamate and glutathione concentrations for adjacent blocks

Mean concentrations, with standard error of means, for glutamate and glutathione across all four fMRS paradigm blocks at TE=60ms (N=12) and TE=100ms (N=12). The p-value of a paired two-sample t-test comparing blocks is also presented. Statistically significant values are bolded.

Concentration time-course plots are shown for glutamate (Figure 2-4) and glutathione (Figure 2-5). Between TE=60ms and TE=100ms, each of the four blocks of the ¹H-fMRS paradigm (Rest, Stroop, Recovery 1, Recovery 2) had significantly different glutamate concentration estimates ($F = 139.756$, d.f. = 1,11, $p < 0.001$). There was no effect of time ($F = 0.876$, d.f. = 3,9, $p = 0.490$) as well as time \times echo time interaction ($F = 1.386$, d.f. = 3,9, $p = 0.309$). Stroop blocks were not significantly different compared to Rest blocks for both TE=60ms ($p = 0.431$, Table 2-4) and TE=100ms ($p = 0.460$, Table 2-4). Similarly, between the two echo times, glutathione concentrations were significantly different ($F = 165.108$, d.f. = 1,11, $p < 0.001$) across all four time-points. No effect of time ($F = 1.748$, d.f. = 3,9, $p = 0.227$) or time \times echo time interaction ($F = 1.836$, d.f. = 3,9, $p = 0.211$) was observed. The Stroop block was significantly different from the Rest block for TE=60ms ($p < 0.05$, Table 2-4) but not for TE=100ms ($p = 0.181$, Table 2-4).

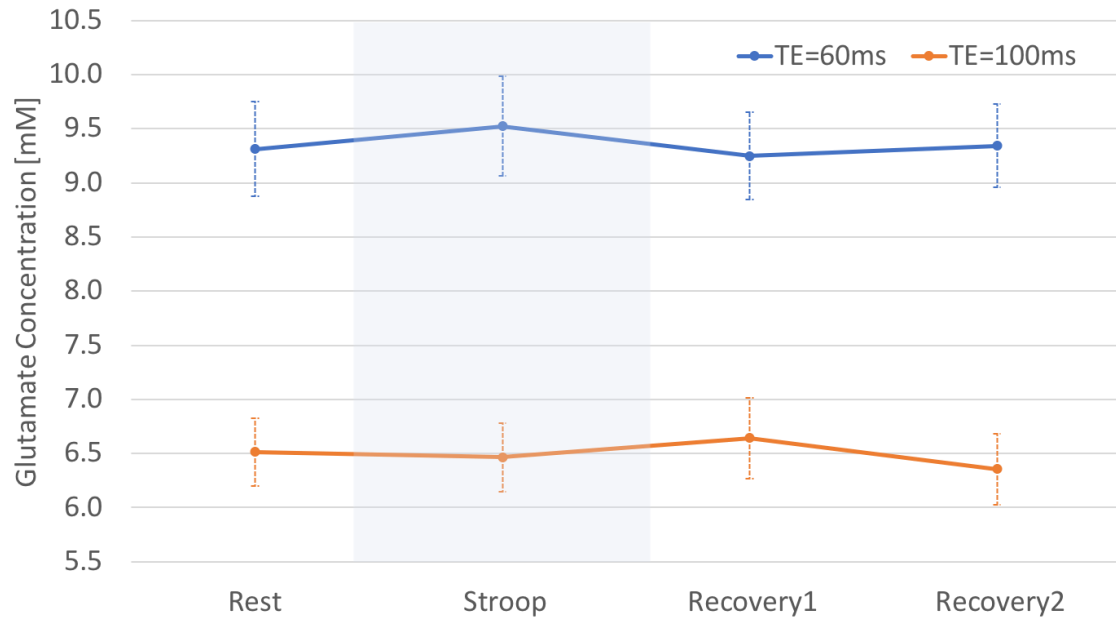


Figure 2-4 Glutamate concentration estimates

Plot of mean concentrations (mM), with standard error of means, of glutamate across the fMRS paradigm at TE=60ms (N=12, *blue*) and TE=100ms (N=12, *orange*). The shaded region highlights the 4 minutes of functional activation using the color-word Stroop task. (Note: the y-axis does not begin at 0 for graphical purposes and may make small absolute differences appear larger.)

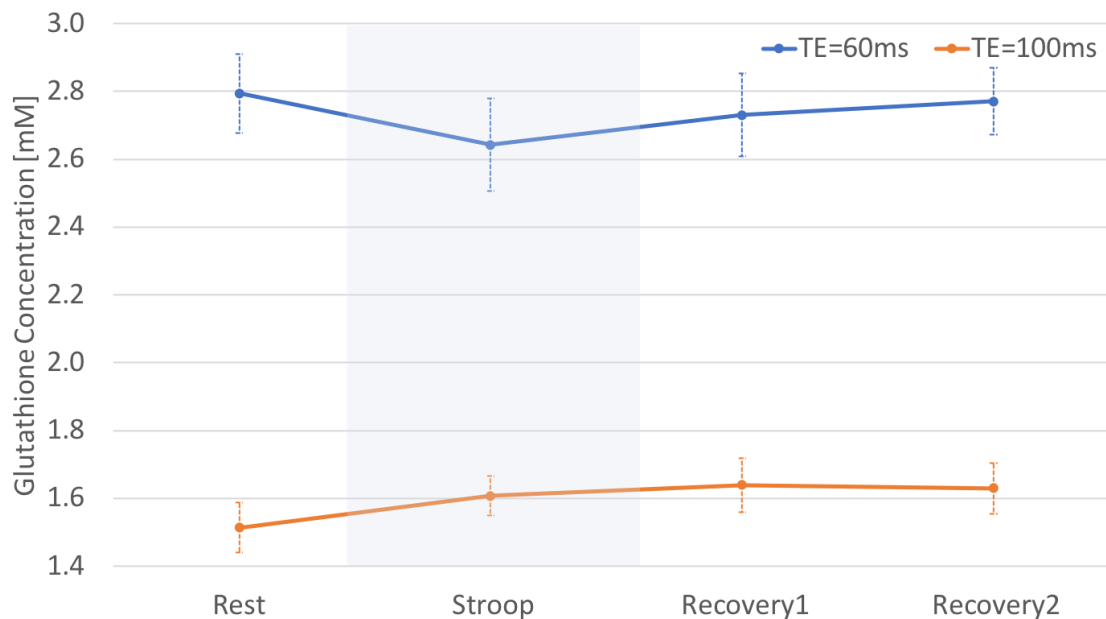


Figure 2-5 Glutathione concentration estimates

Plot of mean concentrations (mM), with standard error of means, of glutathione across the fMRS paradigm at TE=60ms (N=12, blue) and TE=100ms (N=12, orange). The shaded region highlights the 4 minutes of functional activation using the color-word Stroop task. (Note: the y-axis does not begin at 0 for graphical purposes and may make small absolute differences appear larger.)

2.3.3 Metabolite Percentage Changes

Glutamate and glutathione concentration dynamics, relative to resting baseline (block 1), are plotted in Figure 2-6 and Figure 2-7, respectively. Glutamate dynamics were not significantly different across the four blocks between TE=60ms and TE=100ms ($F = 0.541$, d.f. = 1,11, $p = 0.477$). Additionally, no effect of time ($F = 1.819$, d.f. = 2,10, $p = 0.212$) or time \times echo time interaction ($F = 3.170$, d.f. = 2,10, $p = 0.086$) was observed. Glutathione dynamics were significantly different between the two echo times across all time points ($F = 4.939$, d.f. = 1,11, $p < 0.05$). There was no significant effect of time ($F =$

1.971, d.f. = 2,10, $p = 0.190$) or time \times echo time interaction ($F = 0.325$, d.f. = 2,10, $p = 0.730$).

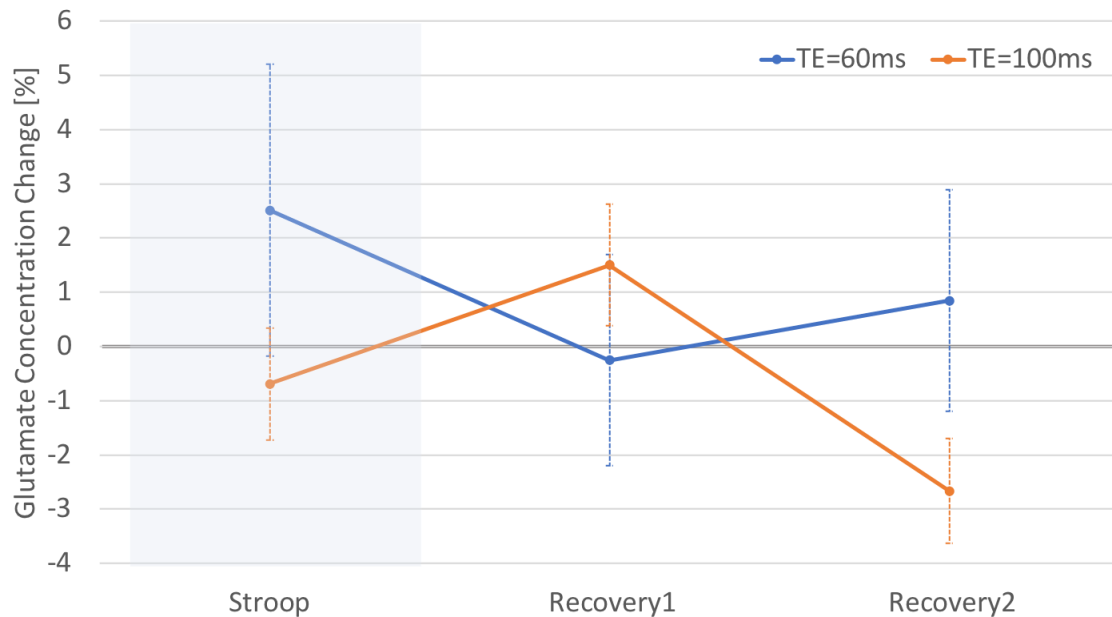


Figure 2-6 Dynamic glutamate concentration changes

Plot of mean concentration changes (%) relative to baseline measurements, with standard error of means, of glutamate across the fMRS paradigm at TE=60ms (N=12, *blue*) and TE=100ms (N=12, *orange*). The shaded region highlights the 4 minutes of functional activation using the color-word Stroop task and the bolded black line indicates the zero line.

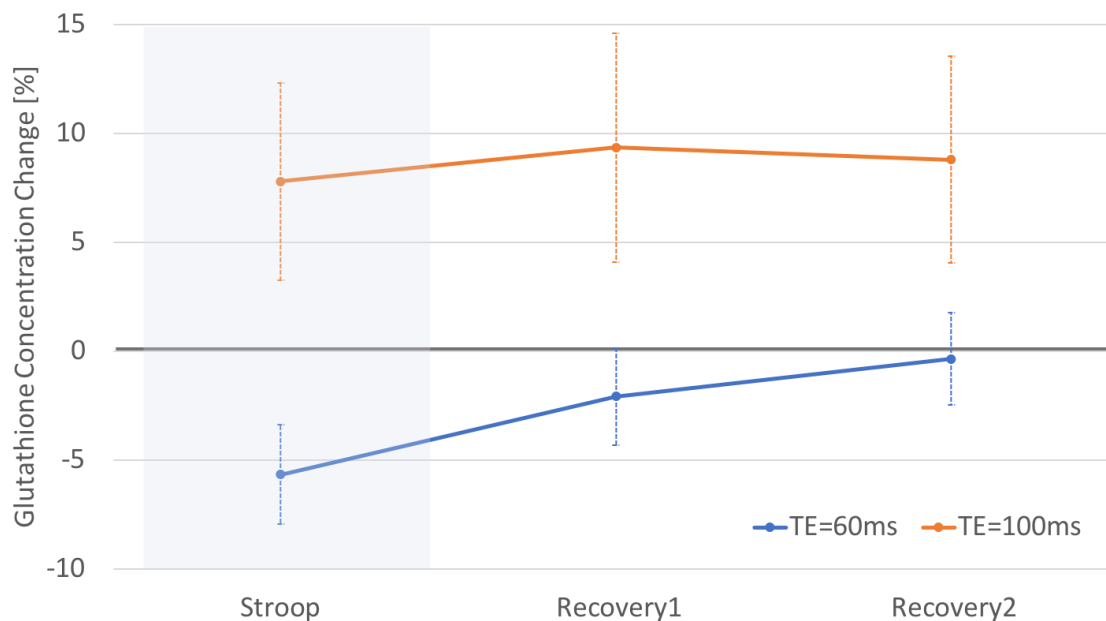


Figure 2-7 Dynamic glutathione concentration changes

Plot of mean concentration changes (%) relative to baseline measurements, with standard error of means, of glutathione across the fMRS paradigm at TE=60ms (N=12, blue) and TE=100ms (N=12, orange). The shaded region highlights the 4 minutes of functional activation using the color-word Stroop task and the black bolded line indicates the zero line.

2.3.4 Metabolite Correlation

A plot of glutamate concentrations versus glutathione concentrations of each individual for all four time-points of the fMRS paradigm are shown in Figure 2-8. Pearson correlation values at TE=60ms for Rest, Stroop, Recovery 1, and Recovery 2 are $r = 0.413$, $p = 0.182$; $r = 0.556$, $p = 0.061$; $r = 0.541$, $p = 0.070$; and $r = 0.615$, $p = 0.033$, respectively. Pearson correlation values at TE=100ms for Rest, Stroop, Recovery 1, and Recovery 2 are $r = 0.859$, $p < 0.001$; $r = 0.555$, $p = 0.061$; $r = 0.654$, $p = 0.021$; and $r = 0.561$, $p = 0.058$, respectively.

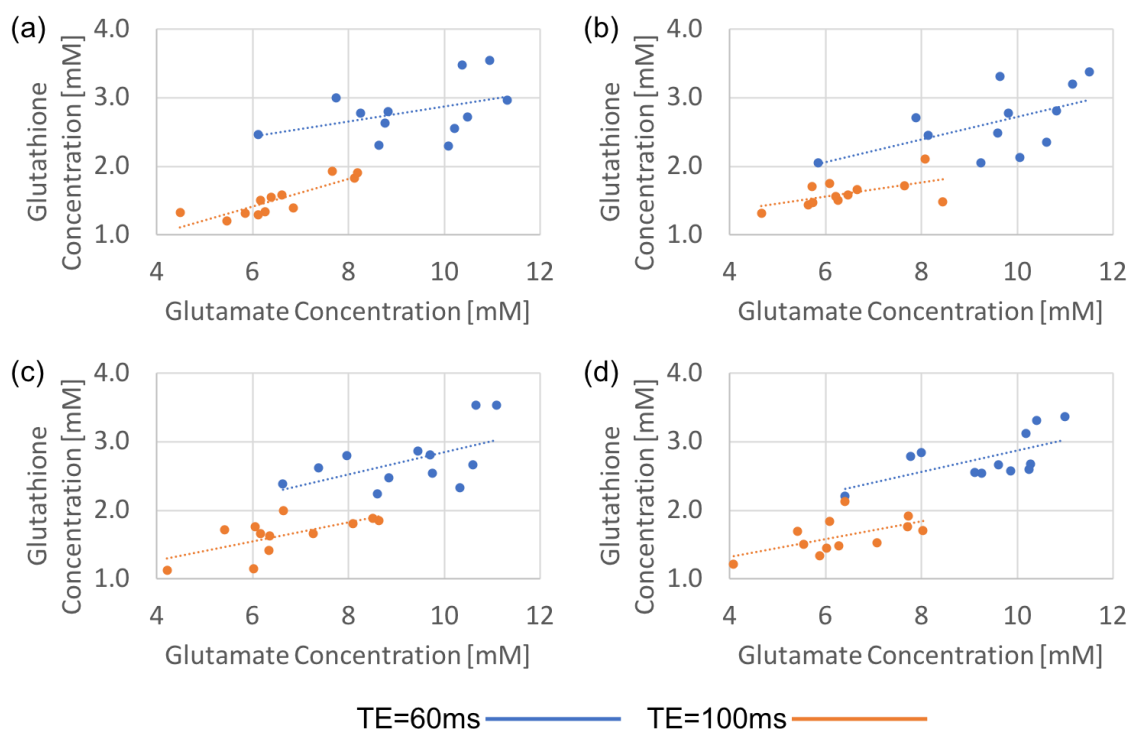


Figure 2-8 Glutamate-glutathione concentration correlation

Correlation between glutamate concentrations (mM) and glutathione concentrations (mM) for (a) Rest, (b) Stroop activation, (c) Recovery 1, and (d) Recovery 2 blocks. Dots indicate individual plots of glutamate versus glutathione concentration and dotted lines represent correlation at TE=60ms (N=12, blue) and TE=100ms (N=12, orange). (Note: the x- and y- axes do not begin at 0 for graphical purposes.)

2.4 Discussion

The main goal of this work was to determine whether a longer echo time or shorter conventional echo time for the semi-LASER MRS sequence would be more appropriate for investigating human brain glutamate and glutathione dynamics in response to a functional task. This work was able to support the finding of Wong *et al.* (2018)¹⁹ that the conventional idea of shortest possible echo times in MRS yielding greatest signal

preserved in metabolite detection is not always true. Although the overall signal detected may be higher for shorter echo times, when studying specific metabolites that have complicated J-coupling evolution, such as glutamate, it is necessary to take into consideration the rephasing of peaks that lead to maxima of signal amplitude at later echo times. This is indeed what was observed as the longer, optimized, echo time (TE=100ms) was just as efficient, if not better, for overall and specific metabolite detection compared to a shorter echo time (TE=60ms). In terms of answering our main objective, the longer echo time was determined more suitable for observing dynamic metabolite levels for several reasons. First, the group coefficients of variation were not statistically different between short and long echo time data. Although this does not directly point towards long echo time superiority, it does provide a strong basis that optimally long echo time MRS does not necessarily mean losing important and valuable signal. Second, the Cramer-Rao lower bound (CRLB) values were significantly lower for glutamate at TE=100ms, with glutathione CRLB values still remaining in acceptable range. Finally, longer echo time MRS has the advantage of fully decayed macromolecular signals, simplifying spectral fitting and quantification and eliminating macromolecular overlap with signal components from other metabolites.

Apart from signal quality, we investigated the viability of our functional MRS tool to confirm that glutamate and glutathione dynamics can be detected using long echo time MRS and that it can provide relevant insight into glutamate and glutathione regulation in the brain. Resting glutamate and glutathione concentrations obtained from this work agreed with current literature²⁷. We observed a significant difference in concentration across all four fMRS paradigm blocks between short and long echo time for both glutamate and glutathione. This is probably partially attributed to macromolecular contribution in the short echo time spectra producing overestimation of metabolites in our spectral fitting and quantification of glutamate and glutathione. Since glutamate and glutathione are metabolites that have small signal contribution, due to amplitude splitting among multiple peaks and low concentration, respectively, overestimation may contribute to significantly different values of concentration estimates. More likely explanations for the significant difference in metabolite concentration between the two echo times are that the spectral quantification approach does not account for metabolite

signal yield or that correction for T_1 and T_2 of voxel tissue compartments may require further improvements.

Positive Pearson correlation observed across all four fMRS paradigm blocks between glutamate concentrations and glutathione concentrations may reflect the brain's normal protective response to increasing oxidative stress resulting from excitatory activation.

Most importantly, dynamic glutamate and glutathione measurements proved to be insightful in studying non-static metabolites in the brain. Upon first look at concentration comparisons of short and long echo time, for both glutamate and glutathione, all time points yielded significant difference in quantification. However, using the resting state measurements to calculate dynamic changes in these metabolites, we found no significant difference in glutamate and glutathione regulation during the fMRS paradigm (except for Stroop block for glutathione).

Limitations of this work include lack of significant activation for glutamate and glutathione during the color-word Stroop task as was demonstrated in our previous work²¹. This may be as a result of using different MRS pulse sequence and parameters for this work as well as having first-episode patient-matched healthy volunteers for this study. Another less likely explanation is that the cognitive Stroop task may not be as stimulating due to quick learning effects in our set of volunteers and may require a stronger functional stimulus to observe significantly detectable change in metabolites. Also, the order of scan (TE=60ms followed by TE=100ms and vice versa) may affect the comparison of metabolite levels between echo times due to what we believe might be a learning effect. Repetition of any task promotes familiarity and can reduce the stimuli effect that we can measure. In our study, 3 of 12 individuals had the TE=60ms scan first followed by the TE=100ms and 9 of 12 individuals had the TE=100ms followed by the TE=60ms. This unbalanced proportion of scan order was due to removing participants from our data set who did not meet one or more of our inclusion criteria for data analysis, and may affect our TE=60ms spectra. An additional limitation of this study was the observation of a quantification accuracy bias possibly due to our approach for determining correction factors for relaxation weighting of the unsuppressed water signal

used as a concentration reference. Inaccurate estimates of water T_1 and T_2 for each tissue at each echo time may explain the noticeable differences observed in concentration estimates between measurements at $TE=60ms$ and $TE=100ms$. Lastly, because every brain looks different, it is not possible to place MRS voxels in precisely the same normalized space in real-time across all participants. It is probable that the voxel placements in this study (and other MRS studies) do not overlap completely but may perhaps be improved using fMRI guidance to include the entire functionally relevant region of the brain.

Future works include application of our long echo time fMRS paradigm in clinically-driven research setting, specifically in first-episode schizophrenia (FES), to investigate if dynamic measurements of glutamate and glutathione can be an effective early marker to help stratify the different subgroups within FES. As well, because fMRS is a relatively novel tool, this work can be extended and refined by increasing the number of participants, especially with a more balanced ratio of echo time scan order. Different stimuli to test activation responses using fMRS is another foreseeable venue of exploration.

2.5 Conclusion

Functional MRS is an exciting tool that still has areas of potential development and refinement for future applications. Our observations will only be as good as the tools we use, especially the right tools. This work was an exploration of attempting to identify the right tools by demonstrating that using optimized long echo time fMRS methods are at least equivalent to conventionally shorter echo time sequences for observing dynamic changes of glutamate and glutathione in the human brain, with the added advantage of simplifying spectral modeling due to removal of macromolecular contribution.

2.6 References

1. Murray RM, Lappin J, Forti M Di. Schizophrenia: From developmental deviance to dopamine dysregulation. *Eur Neuropsychopharmacol.* 2008;18:S129-S134. doi:10.1016/j.euroneuro.2008.04.002
2. Agid O, Remington G, Kapur S, Arenovich T, Zipursky RB. Early Use of Clozapine for Poorly Responding First-Episode Psychosis. *J Clin Psychopharmacol.* 2007;27(4):369-373. doi:10.1097/jcp.0b013e3180d0a6d4
3. Agid O, Schulze L, Arenovich T, et al. Antipsychotic response in first-episode schizophrenia: efficacy of high doses and switching. *Eur Neur.* 2013;23:1017-1022. doi:10.1016/j.euroneuro.2013.04.010
4. Lally J, Ajnakina O, Forti M Di, et al. Two distinct patterns of treatment resistance: clinical predictors of treatment resistance in first-episode schizophrenia spectrum psychoses. *Psychol Med.* 2016;46:3231-3240. doi:10.1017/S0033291716002014
5. Mouchlianitis E, Mccutcheon R, Howes OD. Brain imaging studies of treatment-resistant schizophrenia: a systematic review. *Lancet Psychiatry.* 2016;3(5):451-463. doi:10.1016/S2215-0366(15)00540-4.Brain
6. Javitt DC, Zukin SR. Recent advances in the phenciclidine model of schizophrenia. *Am J Psychiatry.* 1991;148(10):1301-1308. doi:10.1176/ajp.148.10.1301
7. Krystal JH, Karper LP, Seibyl JP, et al. Subanesthetic effects of the noncompetitive NMDA antagonist, ketamine, in humans. Psychotomimetic, perceptual, cognitive, and neuroendocrine responses. *Arch Gen Psychiatry*. 1994;51:199-214.
8. Stone JM, Morrison PD, Pilowsky LS. Glutamate and dopamine dysregulation in schizophrenia – a synthesis and selective review. *J Psychopharmacol.* 2007;21(4):440-452.

9. Egerton A, Brugger S, Raffin M, et al. Anterior cingulate glutamate levels related to clinical status following treatment in first-episode schizophrenia. *Neuropsychopharmacology*. 2012;37(11):2515-2521. doi:10.1038/npp.2012.113
10. Coyle JT. Glutamate and Schizophrenia: Beyond the Dopamine Hypothesis. *Cell Mol Neurobiol*. 2006;26:365-384. doi:10.1007/s10571-006-9062-8
11. Merritt K, Egerton A, Kempton MJ, Taylor MJ, Mcguire PK. Nature of Glutamate Alterations in Schizophrenia A Meta-analysis of Proton Magnetic Resonance Spectroscopy Studies. *JAMA Psychiatry*. 2016;73(7):665-674. doi:10.1001/jamapsychiatry.2016.0442
12. Moghaddam B. Targeting metabotropic glutamate receptors for treatment of the cognitive symptoms of schizophrenia. *Psychopharmacology (Berl)*. 2004;174(1):39-44. doi:10.1007/s00213-004-1792-z
13. Lin C, Lane H. Early Identification and Intervention of Schizophrenia: Insight From Hypotheses of Glutamate Dysfunction and Oxidative Stress. *Front Psychol*. 2019;10:1-9. doi:10.3389/fpsy.2019.00093
14. Liu Z, Zhou T, Ziegler AC, Dimitrion P, Zuo L. Oxidative Stress in Neurodegenerative Diseases: From Molecular Mechanisms to Clinical Applications. *Oxidative Med Cell Longevity*. 2017;2017:1-12.
15. Bitanhirwe BKY, Woo TW. Oxidative stress in schizophrenia : An integrated approach. *Neurosci Biobehav Rev*. 2011;35:878-893. doi:10.1016/j.neubiorev.2010.10.008
16. Prabakaran S, Swatton JE, Ryan MM, et al. Mitochondrial dysfunction in schizophrenia: evidence for compromised brain metabolism and oxidative stress. *Mol Psychiatry*. 2004;9:684-697. doi:10.1038/sj.mp.4001511
17. Anderson KK, Norman R, Macdougall A, et al. Effectiveness of Early Psychosis Intervention : Comparison of Service Users and Nonusers in Population-Based Health Administrative Data. *Am J Psychiatry*. 2018;175:443-452.

doi:10.1176/appi.ajp.2017.17050480

18. McGorry PD, Killackey E, Yung A. Early intervention in psychosis: concepts, evidence and future directions. *World Psychiatry*. 2008;7:148-156.
19. Wong D, Schranz AL, Bartha R. Optimized in vivo brain glutamate measurement using long-echo-time semi-LASER at 7T. *NMR Biomed*. 2018:1-13.
doi:10.1002/nbm.4002
20. Taylor R, Schaefer B, Densmore M, et al. Increased glutamate levels observed upon functional activation in the anterior cingulate cortex using the Stroop Task and functional spectroscopy. *Neuroreport*. 2015;26(3):107-112.
doi:10.1097/WNR.0000000000000309
21. Taylor R, Neufeld RWJ, Schaefer B, et al. Functional magnetic resonance spectroscopy of glutamate in schizophrenia and major depressive disorder: anterior cingulate activity during a color-word Stroop task. *npj Schizophr*. 2015;1:15028.
doi:10.1038/npjSchz.2015.28
22. Peirce J. PsychoPy - psychophysics software in Python. *J Neurosci Methods*. 2007;162(1-2):8-13.
23. Near J, Edden R, Evans CJ, Paquin R, Harris A, Jezzard P. Frequency and Phase Drift Correction of Magnetic Resonance Spectroscopy Data by Spectral Registration in the Time Domain. *Magn Reson Med*. 2015;73(1):44-50.
doi:10.1002/mrm.25094.Frequency
24. Bartha R, Drost DJ, Menon RS, Williamson PC. Spectroscopic Lineshape Correction by QUECC: Combined QUALITY Deconvolution and Eddy Current Correction. *Magn Reson Med*. 2000;44:641-645.
25. Bartha R, Drost DJ, Williamson PC. Factors affecting the quantification of short echo in-vivo 1 H MR spectra: prior knowledge , peak elimination , and filtering. *NMR Biomed*. 1999;12:205-216.

26. IBM C. Released 2016. IBM SPSS Statistics for Windows, Version 24.0. Armonk, NY::IBM Corp.
27. Govindaraju V, Young K, Maudsley AA. Proton NMR chemical shifts and coupling constants for brain metabolites. *NMR Biomed.* 2000;13:129-153. doi:10.1002/1099-1492(200005)13:3<129::AID-NBM619>3.0.CO;2-V
28. Soher B, Semanchuk D, Todd D, Steinberg J, Young K. VeSPA: integrated applications for RF pulse design, spectral simulation and MRS data analysis. *Proc Int Soc Magn Reson Med.* 2011;19(19):1410.

Chapter 3

3 Dynamic glutamate and glutathione measurements in first-episode schizophrenia using 7-Tesla

3.1 Introduction

Schizophrenia is a neurodevelopmental illness that affects the lives of approximately one percent of the population in North America and worldwide^{1,2}. It is characterized by a highly variable combination of positive, negative and cognitive symptoms of varying severity that brings about a sort of uniqueness to each individual with the illness³⁻⁵. While positive symptoms include hallucinations, delusions, and other traits that would otherwise not be present in healthy individuals, negative and cognitive symptoms comprise traits that appear absent or lacking, such as social withdrawal, apathy, lack of emotions, or even difficulty with attention and decision making. Currently, there is no cure for schizophrenia as the etiology and pathophysiological mechanisms of schizophrenia are unclear. Although treatment options do exist, the first line of treatment, often antipsychotics, has only been shown to effectively help manage the positive symptoms of schizophrenia, leaving approximately 30% of individuals with schizophrenia untreated for negative and cognitive symptoms and resistant to initial treatment⁶⁻⁹. The common practice today is that only after several unsuccessful anti-psychotic treatment trials would individuals be regarded as treatment-resistant and prescribed a drug called Clozapine. Clozapine has been shown to be effective in treating the negative and cognitive symptoms of schizophrenia, but due to its adverse side effects, it is often viewed as the last line of treatment⁶. This poses a major challenge because earlier treatment upon onset has been shown to drastically improve patient treatment outcome but presently, there are no tests to definitively know upon first presentation whether someone would be treatment-resistant or not. For treatment-resistant individuals, this translates to delayed effective treatment and having to endure any side effects from the ineffective anti-psychotic drugs.

Looking at neurotransmitter abnormalities has been a great step forward into understanding the possible mechanisms responsible for schizophrenia symptoms¹⁰. For example, dopamine has been found to be clearly involved in schizophrenia as the effectiveness of anti-psychotic medication was found to be correlated with the medication's ability to block D₂ dopamine receptors¹¹. Also, dopamine agonists were found to be able to reproduce major positive symptoms of schizophrenia such as hallucinations and delusions¹². This begs to consider the possibility that other neurotransmitters or brain metabolites could be responsible for the negative and cognitive symptoms of schizophrenia, which would also help us understand why dopamine-based medication seems to be effective mostly for positive symptoms of schizophrenia. Some convincing findings to support this possibility is that Clozapine has a low dopamine receptor occupancy as well as that drugs blocking the N-methyl-D-aspartate (NMDA) glutamate receptors, such as phencyclidine (PCP) and ketamine, are able to reproduce the full range of positive, negative and cognitive symptoms when administered to both healthy individuals and exacerbate the symptoms of those already with schizophrenia^{13,14}.

Two brain metabolites of interest are glutamate and glutathione. Glutamate is the brain's main excitatory neurotransmitter and due to signs of NMDA glutamate receptor involvement in schizophrenia symptoms, has been one of the major metabolites under investigation¹³⁻¹⁵. Glutathione in humans functions as an anti-oxidant and helps reduce oxidative stress. The onset of schizophrenia, typically in adolescence or early adulthood, may be explained by glutamate's involvement in mediating puberty as the main excitatory neurotransmitter¹⁶ with glutathione acting as a physiological reservoir of glutamate neurotransmission^{17,18}.

With the availability of magnetic resonance imaging (MRI) scanners, in-vivo molecular concentrations of brain metabolites can be quantified using a technique called magnetic resonance spectroscopy (MRS). Using the magnetic field strength of the MRI scanner, different brain metabolites will experience extremely small differences in the main field strength due to shielding provided by motion of their own electrons and influence of electron clouds of neighbouring atoms within the same molecule. This small difference is

enough for us to separate and identify the different resonant frequency of signals received from different metabolites.

Much literature has been devoted to using MRS in the study of the brain's major metabolites¹⁹. One difficulty of MRS studies is that some metabolites have overlapping resonances with one another, such as glutamate with glutamine, which makes spectral separation more difficult for accurate quantification^{19,21}. Also, those metabolites that exist in very low concentrations may be hard to detect using low field MRI and so a high-field MRI system provides much benefit for metabolite detection and quantification¹⁹⁻²². Building from standard MRS protocols, functional MRS (fMRS) has been an emerging tool to track changes in brain metabolite in response to an external stimulus^{23,24}. The benefits of fMRS is that since every individual vary in resting brain metabolite levels, it is more appropriate to observe an individual's response based on their own base levels rather than comparing the resting states of individuals within a sample group. Another is that it allows standardization of the activation state during acquisition, which is not traditionally done in standard MRS, and provides more explanatory power regarding underlying metabolic abnormality, while still allowing the traditional comparisons.

The current state of fMRS research shows that the magnitude of changes in metabolite levels can be significantly different based on which stimulus is presented to subjects²⁵⁻²⁸. Hence, when studying schizophrenia or illnesses of the mind, the proper stimulus is necessary that could potentially reveal difference in brain response between individuals who are healthy and ill. A stimulus and response too strong might not reveal much separation or distinction between the two groups, whereas a weak stimulus may not reveal anything at all. Furthermore, when introducing a task, it is necessary that patients can perform almost equally as well as controls so that differences in metabolite levels can be attributed to differences in metabolism rather than performance levels.

This work suggests improvements to previous works as well as offers a novel method for studying glutamate and glutathione in healthy and schizophrenic individuals using fMRS. MRS work usually involves resting states that have been paid little effort to control or standardize the cognitive activity of participants, which may affect metabolite levels even

in the resting state²⁹. Basic fMRI works show that even thoughts of actions, without the action itself, is enough for parts of the brain to be stimulated^{30,31}. This work includes an fMRS protocol with a more controlled cognitive state during both resting and active periods. Secondly, conventional MRS pulse sequences employ a short echo time to minimize J-coupling and T₂ relaxation effects. Along with results from Chapter 2 of this thesis, a recent work suggests and shows that a longer echo time is optimal for glutamate detection for the semi-LASER pulse sequence, adding to the benefit of reduced macromolecular contribution in the acquired spectra³². This work will utilize the optimal echo time for glutamate and glutathione detection. Our team's previous glutamate fMRS work in schizophrenia^{22,26} using a cognitive paradigm incorporated observations from three non-activated blocks interleaved by two activation blocks in medicated patients with schizophrenia. Due to the possible conflicting behaviors of glutamate activation and glutamate recovery from repeated cognitive activation, we proposed extended recovery periods in future works to understand the activated and recovery behaviors more accurately. Building on this past work, we will investigate not only the stimulus response behavior of glutamate and glutathione, but also a prolonged recovery behavior after the stimulus has been removed in never-medicated patients with first-episode schizophrenia.

In this work, we propose an fMRS paradigm using the color-word Stroop task with one activation block and a recovery block that is twice the length of the activation block to observe metabolite recovery behaviors. Based on Taylor *et al.* (2015)'s work²², we predict that the first-episode schizophrenia population will have a reduced and delayed glutamate and glutathione change response to the cognitive task stimulus compared to a healthy control population and that the recovery of both metabolites to baseline be slower in the first-episode schizophrenia population.

3.2 Methods

3.2.1 Participants

Twenty never-medicated first-episode schizophrenia and 25 healthy control volunteers were included in this study. All first-episode schizophrenia volunteers satisfied category

A of DMS-5 Schizophrenia³³ as diagnosed by a psychiatrist and trained assistant and were rated using PANSS-8 scores⁴. Patient volunteers were recruited from PEPP London (Prevention and Early Intervention Program for Psychoses, London, Canada) and healthy control volunteers were recruited through word of mouth while being patient-matched for age, gender and parental socio-economic status. All participants were screened for any other psychiatric disorder, significant head injury, major medical illness, or magnetic resonance imaging (MRI) contraindications and gave informed written consent according to the guidelines of the Human Research Ethics Board for Health Sciences at the University of Western Ontario.

3.2.2 Functional Magnetic Resonance Spectroscopy

Measurements were acquired on a Siemens MAGNETOM 7-Tesla MRI scanner using an 8-channel transmit/ 32-channel receive, head-only, radiofrequency coil at the Centre for Functional and Metabolic Mapping at the University of Western Ontario. A 2.0 x 2.0 x 2.0 cm (8cm³) ¹H-MRS voxel was placed on the bilateral dorsal anterior cingulate cortex (dACC) using a two-dimensional anatomical imaging sequence in the sagittal direction (37 slices, TR=8000ms, TE=70ms, flip-angle (α)=120°, thickness = 3.5mm, field of view = 240×191mm). Voxel positions were set in the area of the dACC where activation was observed based on previous fMRI results that used the same color-word Stroop task²⁶. As well, this area of the brain is part of a larger brain circuit responsible for attention and conflict management, called the basal-ganglia-thalamo-cortical (BGTC) circuit, and is believed to play a role in negative symptoms observed in schizophrenia when circuit abnormalities arise³⁴. A total of 128 channel-combined, water-suppressed spectral averages were acquired using the semi-LASER ¹H-MRS pulse sequence (TR=7500ms, TE=100ms, bandwidth = 6000Hz, N = 2048) during each scan session. Water suppression was achieved using the VAPOR preparation sequence and a water-unsuppressed spectrum was also acquired as a concentration and lineshape deconvolution reference. Prior to each data set acquisition, localized B₀ and B₁ shimming, power and frequency calibrations were made. The functional paradigm implemented had four blocks of spectral acquisition using the color-word Stroop cognitive task. The first block (Rest)

measured resting metabolite levels, the second block (Stroop) measured functional activation in response to the Stroop task, the third block (Recovery 1) measured the recovery behavior of metabolite levels once the Stroop stimulus was removed, and the fourth block (Recovery 2) was an added recovery block to examine the recovery behavior longer. Each block was implemented for four minutes.

3.2.3 Cognitive Stimulus: Color-Word Stroop Task

Before scanning, subjects were introduced to the color-word Stroop task and given specific instructions to follow during the functional magnetic resonance spectroscopy sequence. A four-color (yellow, red, green, blue) button controller was used during the Stroop block of the paradigm for volunteers to respond as quickly as possible to one of the four category words they saw on an image with 50% gray background projected on a screen within the MR scanner: congruent, incongruent, word-only, color-only. Subjects were asked to respond to the color they saw on the screen, regardless of what the actual words spelled out except for the ‘word-only’ category where no color (white text) was presented with the text, in which case, they were asked to respond with the button associated with the color-word. Cognitive stimuli were presented using PsychoPY³⁵ with stimulus presented for 2s followed by cross fixation for 1s, and repeated until the next 4-minute block of the paradigm. All three blocks apart from the Stroop activation block (Rest, Recovery 1, Recovery 2) had full 4-minutes each of cross fixation to standardize the participants’ cognitive state during the resting conditions as much as possible when observing the resting and recovery behaviors of metabolites. Before going into the scanner, all subjects went through a practice trial of the Stroop task in a room adjacent to the MRI suite. To ensure that all participants to be included in the analyses understood the task and could comparably perform it, an 80% response accuracy threshold was set as a requirement during practice trials.

3.2.4 Spectral Post-Processing

Each of the 128 spectral acquisitions was corrected for frequency and phase drifts as described in Near *et al.* (2015)³⁶. The corrected spectra were then averaged according to the fMRS paradigm blocks: the first 32 spectra averaged into one spectrum to represent the entire Rest block, the next 32 spectra for Stroop, and so on for the Recovery 1 and Recovery 2 blocks, to give a total of four final averaged spectra. The final four averaged spectra underwent post-processing using combined QUALITY Eddy Current Correction (QUECC)³⁷, using 400 QUALITY (quantification improvement by converting lineshapes to the Lorentzian type) points, to reduce linewidth distortions as well as Hankel Singular Value Decomposition (HSVD) water removal to remove any residual water signal between 4.2ppm and 5.7ppm before being fit with fitMAN^{32,38}, a time-domain fitting algorithm that uses a non-linear, iterative Levenberg-Marquardt minimization algorithm to echo time-specific prior knowledge templates. The metabolite fitting template included eighteen brain metabolites: alanine, aspartate, choline, creatine, γ -aminobutyric acid (GABA), glucose, glutamate, glutamine, glutathione, glycine, lactate, myo-inositol, N-acetyl aspartate, N-acetyl aspartyl glutamate, phosphorylethanolamine, scyllo-inositol, and taurine. As well, a single peak was used to fit the water unsuppressed spectrum.

Using Barstool³², tissue-specific (gray matter, white matter, and CSF) T_1 and T_2 relaxations were corrected through partial volume segmentation calculations of voxels mapped onto T_1 -weighted images acquired using a 0.75mm isotropic MP2RAGE sequence ($TR=6000ms$, $TI_1=800ms$, $TI_2=2700ms$, flip-angle 1 (α_1)= 4° , flip-angle 2 (α_2)= 5° , $FOV=350mm \times 263mm \times 350mm$, $T_{acq}=9min. 38secs$, $iPAT_{PE}=3$ and $6/8$ k-space). Finally, metabolite concentration quantifications were calculated using the post-processed water suppressed and unsuppressed spectra for each participant along with voxel-appropriate, tissue-specific relaxation time adjustments.

To assess the quality of our acquired data, signal-to-noise ratio (SNR_{NAA}) was calculated by dividing the amplitude of the NAA CH_3 peak in the frequency domain by the standard deviation of the noise in the last 32 most upfield points of the spectrum. The linewidth was also calculated using water-unsuppressed spectra and measuring the full-width-at-half-max (FWHM) of the water peak in Hertz (Hz).

3.2.5 Statistical Analysis

Stroop task accuracy and response times were recorded during scan sessions and were analyzed for differences between groups using a two-sample unequal variance (heteroscedastic) t-test for each of the Stroop categories. Heteroscedastic t-tests were also performed within each group for accuracy and response time to unveil any potential category effects (congruent vs. incongruent).

For the four-spectra block analysis, means and standard deviations of glutamate and glutathione concentrations were calculated for each group. The coefficient of variation was calculated as the ratio of the standard deviation to the mean, expressed as a percentage, for each metabolite within each subject group. Metabolite concentration percentage changes through the fMRS paradigm were calculated as

$$\% \Delta[\text{metabolite}] = \frac{[\text{metabolite}] - [\text{metabolite}]_{\text{baseline}}}{[\text{metabolite}]_{\text{baseline}}} \times 100\%,$$

where $[\text{metabolite}]$ is the concentration of the metabolite at the time of interest during the Stroop paradigm and $[\text{metabolite}]_{\text{baseline}}$ is the concentration of the metabolite acquired from the first post-processed spectral average. Heteroscedastic t-test was performed for each metabolite to compare concentration differences between healthy controls and first-episode schizophrenia at each time point as well as metabolite concentration percentage changes at each time point between the two groups. Two-sample equal variance (homoscedastic) t-tests were used to find any significant changes in absolute metabolite concentration and metabolite concentration percentage changes in relation to time for each metabolite. Lastly, Pearson correlation analysis was used to test the predictability of glutamate change to glutathione change in the fMRS paradigm. All statistics were computed using SPSS³⁹.

3.3 Results

3.3.1 Stroop Task

All participants included in this study were able to meet the 80% accuracy threshold during the Stroop task. Mean accuracy and response times for each of the Stroop categories are shown in Table 3-1. Healthy control volunteers ($M=98.700$, $SD=1.593$) performed the Stroop task with higher accuracy ($t(44) = 4.081$, $p < 0.001$) compared to the first-episode schizophrenia group ($M=94.290$, $SD=5.132$). Both healthy control and patient groups had significantly lower accuracy ($t(48) = 3.438$, $p = 0.001$; $t(40) = 3.726$, $p = 0.001$) in the ‘Incongruent’ category ($M=95.600$, $SD=5.649$; $M=86.430$, $SD=13.242$) compared to the ‘Congruent’ category ($M=99.600$, $SD=1.384$; $M=97.620$, $SD=3.748$). Response times were significantly shorter ($t(44) = -2.817$, $p = 0.007$) for healthy controls ($M=72.117$, $SD=12.121$) compared to first-episode schizophrenia ($M=83.222$, $SD=14.621$), and in both healthy control and patient groups, responding to the ‘Incongruent’ stimuli ($M=1.054$, $SD=0.181$; $M=1.210$, $SD=0.215$) took significantly longer ($t(48) = -4.667$, $p < 0.001$; $t(40) = -3.663$, $p < 0.001$) than responding to the ‘Congruent’ stimuli ($M=0.833$, $SD=0.153$; $M=0.982$, $SD=0.188$).

	<i>HC</i>	<i>FES</i>
<i>Accuracy (%)</i>		
Total	98.7±1.6	94.3±5.1
Congruent	99.6±1.4	97.6±3.7
Incongruent	95.6±5.6	86.4±13.2
Word-Only	99.8±1.0	95.7±4.8
Color-Only	99.8±1.0	97.4±5.2
<i>Response Time (s)</i>		
Total	72.1±12.1	83.2±14.6
Congruent	0.83±0.15	0.98±0.19
Incongruent	1.05±0.18	1.21±0.22
Word-Only	0.91±0.16	1.06±0.20
Color-Only	0.81±0.14	0.91±0.17

Table 3-1 Summary of Stroop task performance

Mean accuracy (%) and response time (s), with standard deviation, for healthy controls (N=25) and first-episode schizophrenia (N=21). Values are given for total mean as well as each of the Stroop categories.

3.3.2 Spectral Quality and Fit

An example of voxel positioning on the bilateral dorsal ACC can be seen in Figure 3-1 as well as a sample spectral fit using the fitMAN software in Figure 3-2. Individual metabolite spectra are also shown for metabolites of interest.

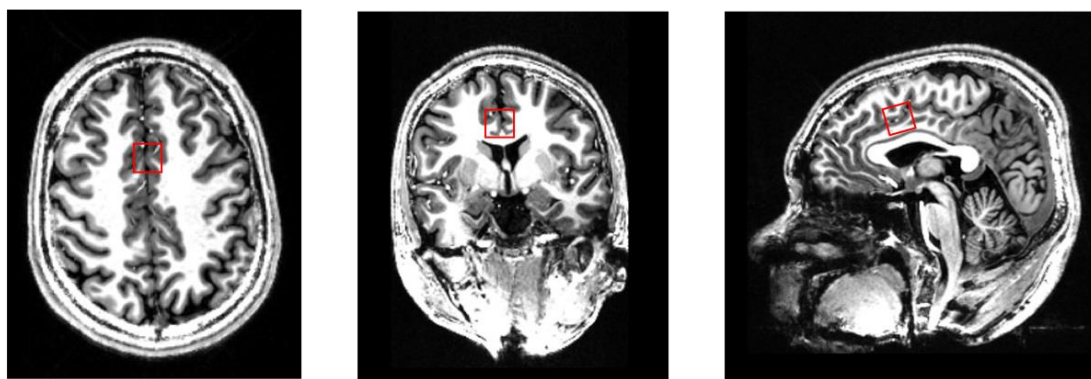


Figure 3-1 Voxel position

A 2cm x 2cm x 2cm voxel (*red*) placed in the dorsal anterior cingulate cortex (ACC) in the transverse (*left*), coronal (*middle*), and sagittal (*right*) view.

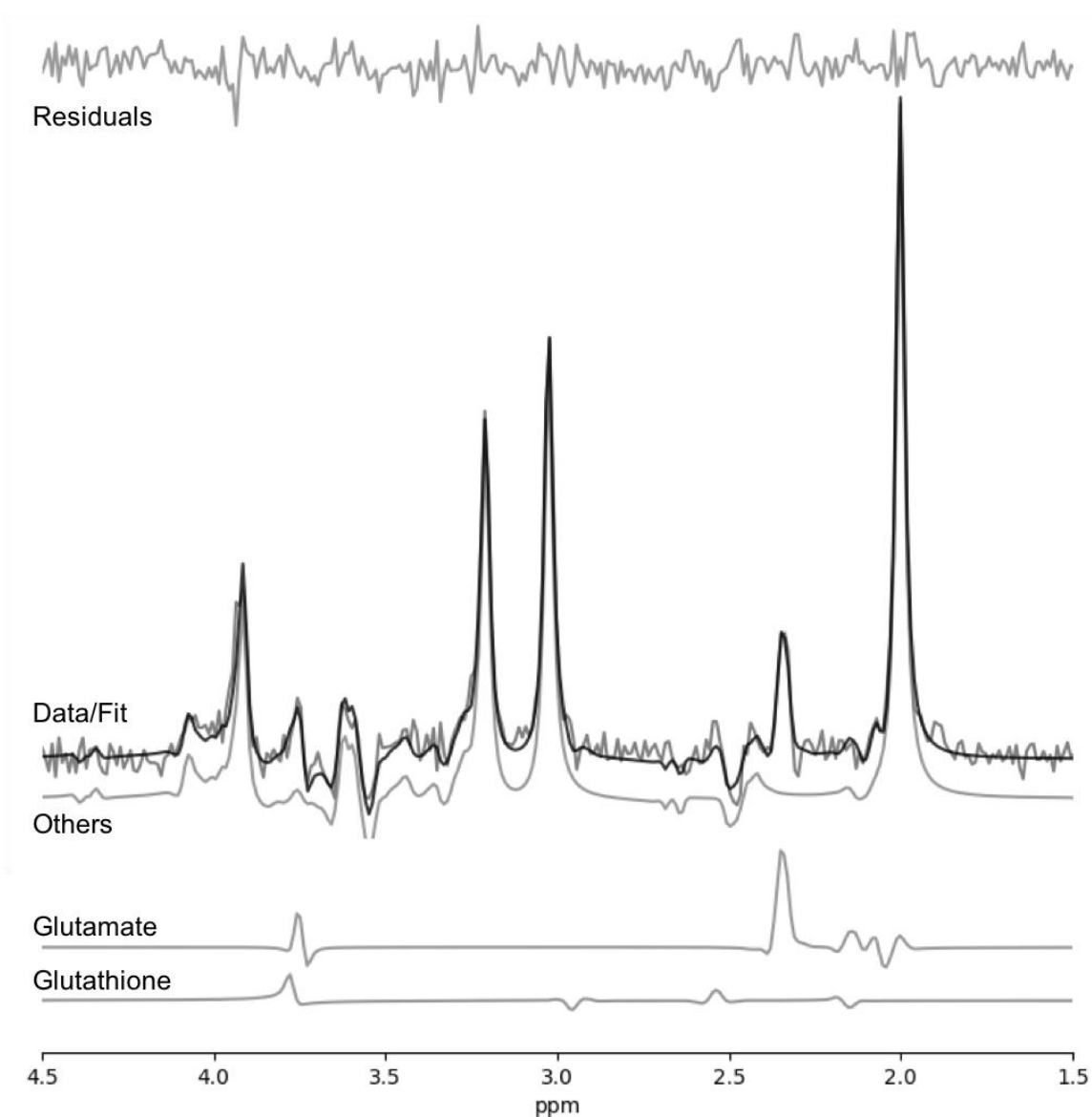


Figure 3-2 Spectral fit with metabolite components

Sample spectral fit using fitMAN. The bolded black line represents the final fit spectrum overlaid on the raw data (light grey) from a first-episode schizophrenia participant of this study. Individual spectral components of metabolites of interest are shown below the fitted spectrum. A 1Hz exponential filter was applied for display only.

Spectral quality assessments were made using SNR_{NAA} (Table 3-2), water spectral linewidth (Table 3-2), coefficient of variation (Table 3-3), and Cramer-Rao lower bounds (Table 3-4). There was no significant difference in SNR_{NAA} ($t(44) = 0.280$, $p = 0.780$) or linewidth ($t(44) = -1.270$, $p = 0.211$) between the healthy control and first-episode schizophrenia groups. Coefficient of variation values were only significantly different between healthy control and first-episode schizophrenia groups in the Recovery 2 block for glutathione ($p < 0.005$, $F=0.28$). Lastly, there were no significant differences ($t(182) = -1.316$, $p = 0.190$; $t(182) = -0.416$, $p = 0.678$) between healthy controls ($M=3.109$, $SD=0.535$; $M=9.127$, $SD=1.956$) and first-episode schizophrenia cohorts ($M=3.218$, $SD=0.602$; $M=9.238$, $SD=1.609$) for glutamate and glutathione CRLB values, respectively.

<i>Group</i>	SNR_{NAA}	LW_W
<i>HC</i>	219±57	7.0±1.2 Hz
<i>FES</i>	214±51	7.4±1.0 Hz

Table 3-2 Signal-to-noise ratio (SNR_{NAA}) and linewidth (LW_W)

Mean SNR_{NAA} and LW_W , with standard deviation, for healthy control (N=25) and first-episode schizophrenia (N=21) groups.

<i>Group</i>	<i>Rest</i>	<i>Stroop</i>	<i>Recovery1</i>	<i>Recovery2</i>
<i>HC</i>				
[Glu]	14.4	15.0	15.3	15.4
[GSH]	17.0	13.2	17.8	11.5
<i>FES</i>				
[Glu]	18.2	19.1	20.1	18.6
[GSH]	21.1	15.0	20.0	22.2
<i>HC vs FES</i>				
[Glu]	$p = 0.28 (F = 0.63)$	$p = 0.27 (F = 0.62)$	$p = 0.21 (F = 0.59)$	$p = 0.39 (F = 0.69)$
[GSH]	$p = 0.33 (F = 0.66)$	$p = 0.55 (F = 0.78)$	$p = 0.59 (F = 0.80)$	$p = \mathbf{0.003 (F = 0.28)}$

Table 3-3 Summary of coefficients of variation (CV)

Glutamate and glutathione coefficients of variation expressed as a percentage (%) for healthy control (HC) and first-episode schizophrenia (FES) groups. Comparison of inter-individual CV between the two groups are shown for each fMRS paradigm block. Statistically significant values are bolded.

<i>Group</i>	<i>CRLB (%)</i>
<i>HC</i>	
[Glu]	3.11±0.05
[GSH]	9.13±0.20
<i>FES</i>	
[Glu]	3.22±0.07
[GSH]	9.24±0.18

Table 3-4 Cramer-Rao lower bound (CRLB) values

Mean CRLB values, expressed as a percentage (%), with standard deviations, from glutamate and glutathione concentration calculations for healthy control (N=25) and first-episode schizophrenia (N=21) groups.

3.3.3 Metabolite Concentration

Table 3-5 summarizes the glutamate and glutathione concentrations across the four fMRS blocks. A pairwise comparison of adjacent blocks revealed significant decreases in glutamate concentration between Recovery 1 (M=6.597, SD=1.012) and Recovery 2 (M=6.462, SD=0.997) in healthy controls ($t(24) = 2.666$, $p = 0.014$) as well as between Stroop (M=6.947, SD=1.328) and Recovery 1 (M=6.767, SD=1.360) in the first-episode schizophrenia group ($t(20) = 2.718$, $p = 0.013$). There was also a significant increase in glutathione concentration between Rest (M=1.482, SD=0.252) and Stroop (M=1.605, SD=0.212) for healthy controls ($t(24) = -2.819$, $p = 0.009$). Strong trend toward increasing glutamate levels was present between Rest (M=6.809, SD=1.238) and Stroop (M=6.947, SD=1.328) of first-episode schizophrenia cohorts ($t(2) = -1.887$, $p = 0.074$) as well as a strong trend toward decreasing glutathione levels between Recovery 1 (M=1.667, SD=0.297) and Recovery 2 (M=1.577, SD=0.182) in healthy controls ($t(24) = 1.954$, $p = 0.062$).

<i>Group</i>	<i>p(Stroop- Rest)</i>	<i>p(Rec1- Stroop)</i>	<i>p(Rec1- Rec2)</i>	<i>Rest</i>	<i>Stroop</i>	<i>Recovery1</i>	<i>Recovery2</i>
<i>HC</i>							
[Glu]	0.566	0.534	0.014	6.61±0.19	6.63±0.20	6.60±0.20	6.46±0.20
[GSH]	0.009	0.255	0.062	1.48±0.05	1.61±0.04	1.67±0.06	1.56±0.04
<i>FES</i>							
[Glu]	0.074	0.013	0.166	6.81±0.27	6.95±0.29	6.77±0.30	6.67±0.27
[GSH]	0.417	0.508	0.985	1.74±0.08	1.69±0.06	1.65±0.07	1.65±0.08

Table 3-5 Pairwise comparison of glutamate and glutathione concentrations

Mean concentrations, with standard error of means, for glutamate and glutathione across all four fMRS paradigm blocks for healthy control (N=25) and first-episode schizophrenia (N=21) groups. Comparison between adjacent blocks are given between the blocks. Statistically significant values are bolded.

Time-course plots of glutamate and glutathione concentrations are shown in Figure 3-3 and figure 3-4, respectively. Significantly higher resting glutathione concentration ($t(44) = -2.784, p = 0.008$) was observed in first-episode schizophrenia ($M=1.736, SD=0.366$) compared to healthy controls ($M=1.482, SD=0.252$).

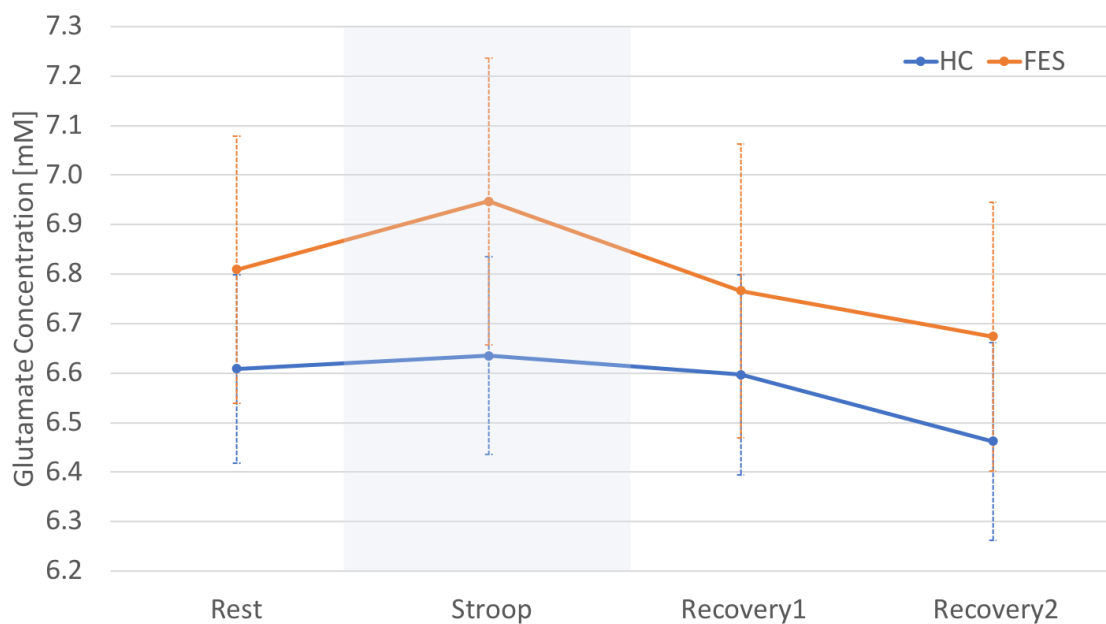


Figure 3-3 fMRS glutamate concentration time-course

Plot of mean concentrations (mM), with standard error of means, of glutamate across the fMRS paradigm for HC (N=25, blue) and FES (N=21, orange). The shaded region highlights the 4 minutes of functional activation using the color-word Stroop task. (Note: the y-axis does not begin at 0 for graphical purposes.)

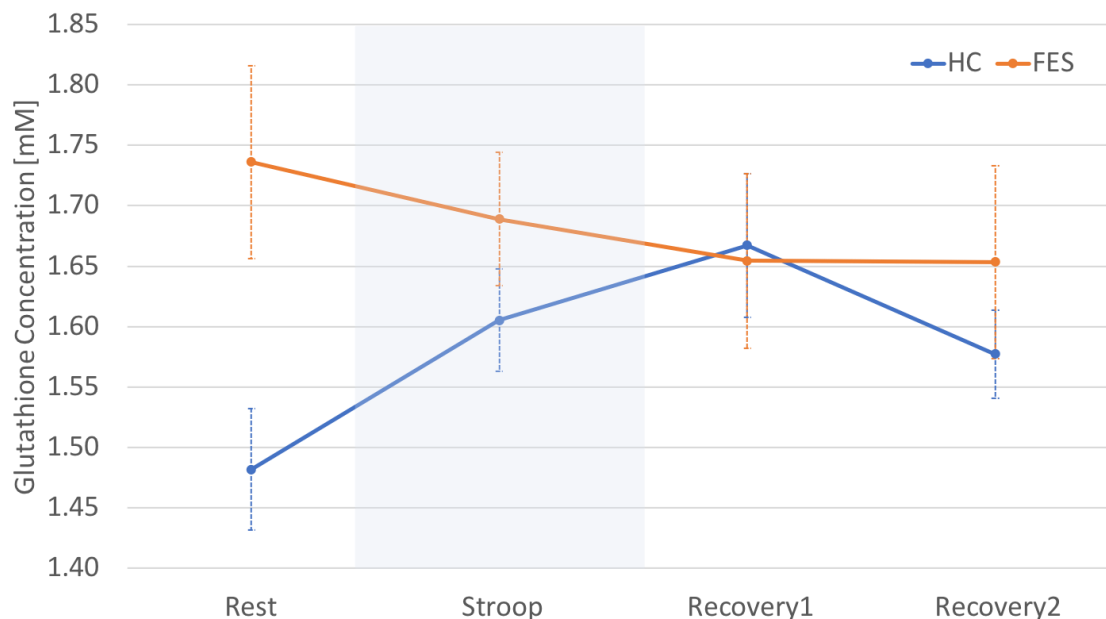


Figure 3-4 fMRS glutathione concentration time-course

Plot of mean concentrations (mM), with standard error of means, of glutathione across the fMRS paradigm for HC (N=25, blue) and FES (N=21, orange). The shaded region highlights the 4 minutes of functional activation using the color-word Stroop task. (Note: the y-axis does not begin at 0 for graphical purposes.)

3.3.4 Metabolite Dynamics

Glutamate dynamics, relative to resting baseline, showed no significant group difference between healthy control and first-episode schizophrenia (Figure 3-5). However, healthy controls had significantly higher glutathione concentration changes compared to the first-episode schizophrenia group (Figure 3-6) across all non-resting fMRS blocks: Stroop ($t(44) = 2.322$, $p = 0.025$), Recovery 1 ($t(44) = 2.908$, $p = 0.006$), and Recovery 2 ($t(44) = 2.926$, $p = 0.005$).

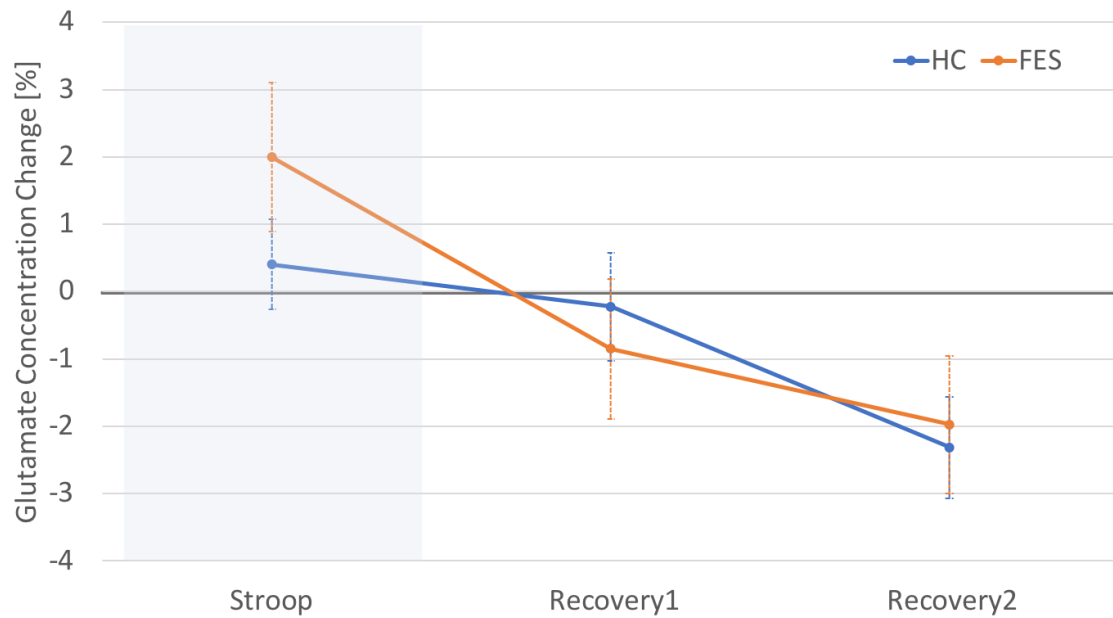


Figure 3-5 fMRS glutamate dynamics

Plot of mean concentration changes (%) relative to baseline measurements, with standard error of means, of glutamate across the fMRS paradigm for HC (N=25, *blue*) and FES (N=21, *orange*). The shaded region highlights the 4 minutes of functional activation using the color-word Stroop task.

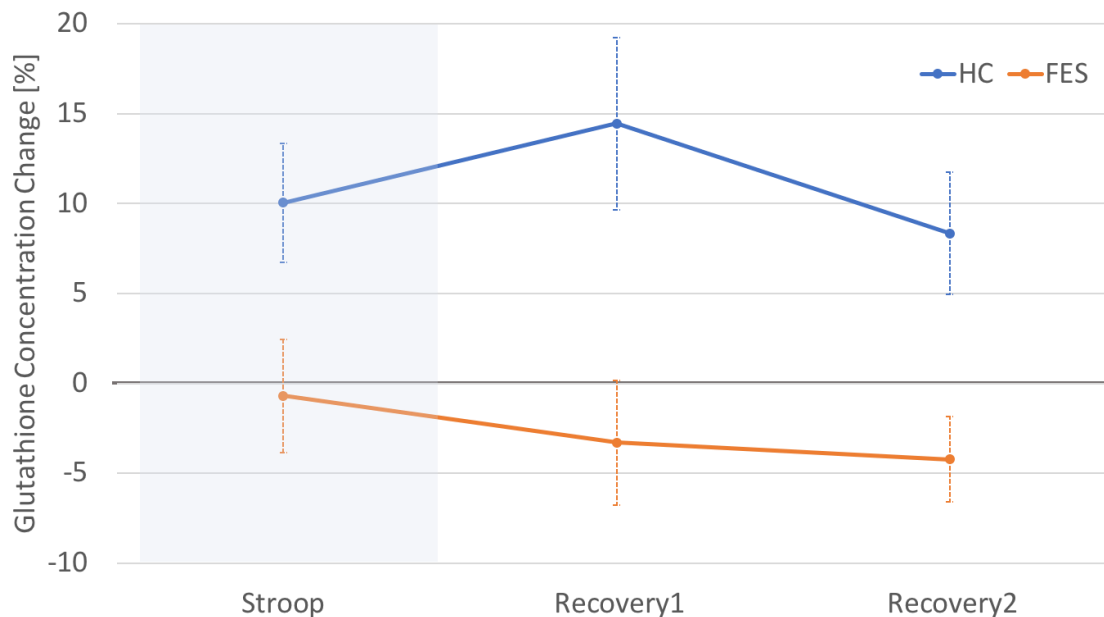


Figure 3-6 fMRS glutathione dynamics

Plot of mean concentration changes (%) relative to baseline measurements, with standard error of means, of glutathione across the fMRS paradigm for HC (N=25, *blue*) and FES (N=21, *orange*). The shaded region highlights the 4 minutes of functional activation using the color-word Stroop task.

3.3.5 Correlation Analysis

Figure 3-7 show plots of glutamate versus glutathione concentrations of each individual for the four fMRS blocks. Pearson correlation values for healthy controls for Rest, Stroop, Recovery 1, and Recovery 2 are $r = 0.603$, $p = 0.001$; $r = 0.448$, $p = 0.025$; $r = 0.507$, $p = 0.010$; and $r = 0.521$, $p = 0.008$, respectively. Pearson r for the first-episode schizophrenia group for Rest, Stroop, Recovery 1, and Recovery 2 are $r = 0.700$, $p < 0.001$; $r = 0.724$, $p < 0.001$; $r = 0.842$, $p < 0.001$; and $r = 0.818$, $p < 0.001$, respectively.

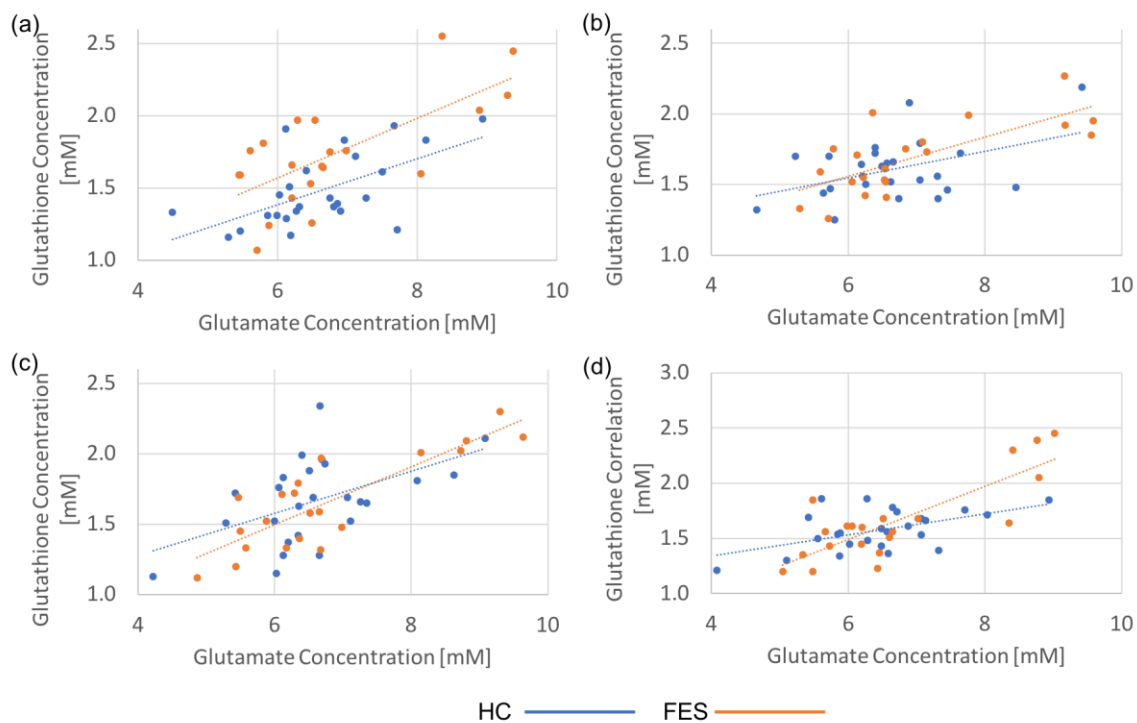


Figure 3-7 Correlation of glutamate and glutathione concentrations

Correlation between glutamate concentrations (mM) and glutathione concentrations (mM) for (a) Rest, (b) Stroop activation, (c) Recovery 1, and (d) Recovery 2 blocks. Dots indicate individual plots of glutamate versus glutathione concentration and dotted lines represent correlation for HC (N=25, blue) and FES (N=21, orange). (Note: the x- and y- axes do not begin at 0 for graphical purposes.)

3.4 Discussion

3.4.1 Glutamate and Glutathione Concentration

This current study builds upon previous work^{22,26} to investigate possible glutamate and glutathione regulation abnormalities in the brain of first-episode schizophrenia cohorts using a dynamic tool, functional MRS. Our findings indicate that fMRS is more appropriate than simple resting state MRS for looking at brain metabolites that are highly dynamic.

Resting glutamate levels were higher, but not significantly, in FES than HC ($t(44) = -0.621, p = 0.538$). We did not observe a significant increase in glutamate levels in either HC ($t(24) = -0.582, p = 0.566$) or FES ($t(20) = -1.887, p = 0.074$) in response to the color-word Stroop task. However, a strong trend toward increased glutamate in FES during the functional task ($t(20) = -1.887, p = 0.074$), a significant decrease in glutamate from the Stroop block to the Recovery 1 block ($t(20) = 2.718, p = 0.013$) where glutamate levels returned to near baseline values, as well as visual observation of Figure 3-3 suggests that stronger activation was present in FES than HC. This is also supported by the Stroop performance where HC performed significantly more accurately ($t(44) = 4.081, p < 0.001$) and quickly ($t(44) = -2.817, p = 0.007$) than their FES counterparts across all categories of the color-word Stroop task. Also, interesting glutamate behavior was observed in the recovery periods of both HC and FES. As predicted, once the functional stimulus was removed, glutamate levels returned to baseline levels by the first recovery period for both groups. However, glutamate concentrations continued to fall during the second recovery period, falling significantly lower than baseline values for HC ($t(24) = 3.053, p = 0.005$). This is a behavior not yet cited in current literature and perhaps need further exploration. One theory behind this occurrence may be a predictive compensation effect of the brain's preparation for subsequent, or near-future, stimuli activation, which may lead to excitotoxicity from glutamate response.

Glutathione levels at rest were found to be significantly higher ($t(44) = -2.784, p = 0.008$) in our FES group ($M=1.736, SD=0.366$) than in HC ($M=1.482, SD=0.252$), suggesting higher than normal levels of oxidative stress present in FES. Furthermore, significant increase in glutathione concentration in HC ($t(24) = -2.819, p = 0.009$) but not in FES ($t(20) = 0.828, p = 0.417$) may point toward abnormal FES glutathione regulation and response to oxidative stress from repeated cognitive tasks.

3.4.2 Dynamic Changes in Glutamate and Glutathione

Changes in glutamate levels for FES (~2% concentration increase) during the color-word Stroop task agree with our own past work using a different pulse sequence²². When

looking at the dynamic glutamate recovery period, we observe an approximately similar 2% drop in glutamate levels no matter how much or little activation was present during the Stroop block for both HC and FES. This additional feature of glutamate recovery may further support the suggestion for a predictive compensation effect in the brain. By anticipating subsequent cognitive battery from initial stimulus presentation, the brain may lower its glutamate levels as an adaptive response to prevent potential excitotoxicity from stimulus-induced glutamate excess.

The fMRS measurements of glutathione show more dramatic changes during the task paradigm conditions, suggesting that traditional MRS methods would not capture this information and be confounded by such dynamic effects, making their interpretation even more difficult. Healthy controls responded strongly (~10% glutathione concentration increase) to the functional task and presumed associated oxidative stress, and continued to remain at high levels even after the functional stimulus was removed. This behavior complements possible compensation effects of glutamate, reflecting the brain's possible short-term preparation for further stimuli in the near-future by keeping glutathione levels active. First-episode schizophrenia glutathione dynamics revealed the opposite, starting and continuing decline in glutathione levels, strongly suggesting FES participants' lack of proper glutathione response and mitigation of oxidative stress.

3.4.3 Correlation

Positive correlation was observed between glutamate and glutathione concentrations across all four fMRS blocks (Section 3.3.5). Specifically, the resting state correlation is in alignment with findings of Kumar *et al.* (2018)⁴⁰. We also found that the FES group exhibited much stronger correlation across all time points compared to HC, especially during the Recovery 1 period ($z = -2.07$, $p < 0.05$) and Recovery 2 period ($z = -1.83$, $p = 0.07$). One possibility to explain our correlation findings would be that an already elevated level of glutamate, especially in FES, may lead to active oxidation of glutamate into glutathione in a self-regulation attempt to prevent excitotoxicity.

3.4.4 Limitations and Future Work

Several limitations should be addressed. First, lack of significant glutamate activation and minor discrepancies compared to previous work²² may be due to the completely different MRS sequence used for this study (semi-LASER vs STEAM), as well as having our echo time optimized for glutamate detection (based on work from Chapter 2) as opposed to conventional short echo time parameters. We also note that never-medicated first-episode schizophrenia cohorts in this study reflect a different volunteer recruitment pool than our previous study (individuals with chronic schizophrenia, with medication)²², and may affect our observations. Finally, although 21 FES participants were included in this study, our FES population was not divided by any symptom or treatment category. It is quite possible that within different categories, such as dopamine-based first-line medication responders versus non-responders, or even among affected symptom groups, we may see new trends and findings of abnormal glutamate and glutathione regulation and behavior in FES.

Future work will include using follow-up assessment and scan data to retrospectively group our current fMRS data into appropriate sub-groups. This will reveal if glutamate and/or glutathione abnormalities can be used as effective early markers for treatment response outcome in first-episode schizophrenia. Another area to investigate further is the glutamate recovery behavior mentioned in our analysis. Seeing glutamate levels drop below resting levels after extended recovery period in both HC and FES has never been assessed and may reveal insight into glutamate regulation in response to functional tasks in the human brain while the rest and active period serve more as cognitive status standardization. Understanding brain glutamate and glutathione dynamics is crucial in designing proper protocols of study observation and proper physiological models of how their bulk tissue concentration varies during activation⁴¹.

3.5 Conclusion

In order to be sensitive to metabolite dynamics in the human brain, functional MRS measurements are more appropriate than traditional MRS, especially if levels of brain activity during the acquisition are not properly controlled. Although fMRS methodology is still developing, this work was able to highlight insightful glutamate behavior as well as abnormal glutathione behavior in first-episode schizophrenia. This work is one step closer to finding appropriate early markers for symptom treatment outcome in schizophrenia so that the right medication can be administered to the right patient upon first presentation into the clinic.

3.6 References

1. Saha S, Chant D, Welham J, Mcgrath J. A Systematic Review of the Prevalence of Schizophrenia. *PLoS Med.* 2005;2(5):413-433. doi:10.1371/journal.pmed.0020141
2. Moreno-Kustner B, Martin C, Pastor L. Prevalence of psychotic disorders and its association with methodological issues . A systematic review and meta-analyses. *PLoS One.* 2018;13(4):1-25.
3. Kay SR, Sevy S. Pyramidal model of schizophrenia. *Schizophr Bull.* 1990;16(3):537-545. doi:10.1093/schbul/16.3.537
4. Kay SR, Fiszbein A, A OL. The Positive and Negative Syndrome Scale (PANSS) for Schizophrenia. *Schizophr Bull.* 1987;13(2):261-276.
5. Liddle PF. The Symptoms of Chronic Schizophrenia: A Re-examination of the Positive-Negative Dichotomy. *Br J Psychiatry.* 1987;151:145-151.
6. Agid O, Remington G, Kapur S, Arenovich T, Zipursky RB. Early Use of Clozapine for Poorly Responding First-Episode Psychosis. *J Clin Psychopharmacol.* 2007;27(4):369-373. doi:10.1097/jcp.0b013e3180d0a6d4
7. Agid O, Schulze L, Arenovich T, et al. Antipsychotic response in first-episode schizophrenia: efficacy of high doses and switching. *Eur Neur.* 2013;23:1017-1022. doi:10.1016/j.euroneuro.2013.04.010
8. Lally J, Ajnakina O, Forti M Di, et al. Two distinct patterns of treatment resistance: clinical predictors of treatment resistance in first-episode schizophrenia spectrum psychoses. *Psychol Med.* 2016;46:3231-3240. doi:10.1017/S0033291716002014
9. Mouchlianitis E, Mccutcheon R, Howes OD. Brain imaging studies of treatment-resistant schizophrenia: a systematic review. *Lancet Psychiatry.* 2016;3(5):451-463. doi:10.1016/S2215-0366(15)00540-4.Brain

10. Lin C, Lane H. Early Identification and Intervention of Schizophrenia: Insight From Hypotheses of Glutamate Dysfunction and Oxidative Stress. *Front Psychol.* 2019;10:1-9. doi:10.3389/fpsy.2019.00093
11. Murray RM, Lappin J, Forti M Di. Schizophrenia: From developmental deviance to dopamine dysregulation. *Eur Neuropsychopharmacol.* 2008;18:S129-S134. doi:10.1016/j.euroneuro.2008.04.002
12. Seeman P. Dopamine Receptors and the Dopamine Hypothesis of Schizophrenia. *Synapse.* 1987;1:133-152.
13. Javitt DC, Zukin SR. Recent advances in the phenciclidine model of schizophrenia. *Am J Psychiatry.* 1991;148(10):1301-1308. doi:10.1176/ajp.148.10.1301
14. Krystal JH, Karper LP, Seibyl JP, et al. Subanesthetic effects of the noncompetitive NMDA antagonist, ketamine, in humans. Psychotomimetic, perceptual, cognitive, and neuroendocrine responses. *Arch Gen Psychiatry*. 1994;51:199-214.
15. Javitt DC. Glutamatergic theories of schizophrenia. *Isr J Psychiatry Relat Sci.* 2010;47(1):4-16.
16. Giuliani FA, Escudero C, Casas S, Bazzocchini V, Yunes R, Laconi MR. Allopregnanolone and puberty: modulatory effect on glutamate and GABA release and expression of 3alpha-hydroxysteroid oxidoreductase in the hypothalamus of female rats. *Neuroscience.* 2013;243:64-75. doi:10.1016/j.neuroscience.2013.03.053
17. Sedlak TW, Paul BD, Parker GM, Hester LD, Taniguchi Y, Kamiya A, Snyder SH, Sawa A. The glutathione cycle shapes synaptic glutamate activity. *PNAS.* 2019;116(7):2701-2706. doi:10.1073/pnas.1817885116
18. Liu Z, Zhou T, Ziegler AC, Dimitrion P, Zuo L. Oxidative Stress in Neurodegenerative Diseases: From Molecular Mechanisms to Clinical

- Applications. *Oxidative Med Cell Longevity*. 2017;2017:1-12.
19. Govindaraju V, Young K, Maudsley AA. Proton NMR chemical shifts and coupling constants for brain metabolites. *NMR Biomed*. 2000;13:129-153. doi:10.1002/1099-1492(200005)13:3<129::AID-NBM619>3.0.CO;2-V
 20. Penner J, Bartha R. Semi-LASER ^1H MR Spectroscopy at 7 Tesla in Human Brain: Metabolite Quantification Incorporating Subject-Specific Macromolecule Removal. *Magn Reson Med*. 2015;74:4-12. doi:10.1002/mrm.25380
 21. Tkac I, Oz G, Adriany G, Ugurbil K, Gruetter R. In Vivo ^1H NMR Spectroscopy of the Human Brain at High Magnetic Fields: Metabolite Quantification at 4T vs. 7T. *Magn Reson Med*. 2009;62(4):868-879. doi:10.1002/mrm.22086.In
 22. Taylor R, Neufeld RWJ, Schaefer B, et al. Functional magnetic resonance spectroscopy of glutamate in schizophrenia and major depressive disorder: anterior cingulate activity during a color-word Stroop task. *npj Schizophr*. 2015;1:15028. doi:10.1038/npjSchz.2015.28
 23. Mullins PG. Towards a theory of functional magnetic resonance spectroscopy (fMRS): A meta-analysis and discussion of using MRS to measure changes in neurotransmitters in real time. *Scand J Psychol*. 2018;59:91-103. doi:10.1111/sjop.12411
 24. Woodcock EA, Anand C, Khatib D, Diwadkar VA, Stanley JA. Working Memory Modulates Glutamate Levels in the Dorsolateral Prefrontal Cortex during ^1H fMRS. *Front Psychiatry*. 2018;9(66):1-10. doi:10.3389/fpsy.2018.00066
 25. Mangia S, Tka I, Gruetter R, Moortele P-F Van de, Maraviglia B, Ugurbil K. Sustained neuronal activation raises oxidative metabolism to a new steady-state level : evidence from ^1H NMR spectroscopy in the human visual cortex. *J Cereb Blood Flow Metab*. 2007;27:1055-1063. doi:10.1038/sj.jcbfm.9600401
 26. Taylor R, Schaefer B, Densmore M, et al. Increased glutamate levels observed upon functional activation in the anterior cingulate cortex using the Stroop Task

- and functional spectroscopy. *Neuroreport*. 2015;26(3):107-112.
doi:10.1097/WNR.0000000000000309
27. Mullins PG, Rowland TLM, Jung RE, Sibbitt WL. A novel technique to study the brain's response to pain: Proton magnetic resonance spectroscopy. *Neuroimage*. 2005;26:642-646. doi:10.1016/j.neuroimage.2005.02.001
 28. Gussew A, Rzanny R, Erdtel M, et al. Time-resolved functional 1H MR spectroscopic detection of glutamate concentration changes in the brain during acute heat pain stimulation. *Neuroimage*. 2010;49:1895-1902.
doi:10.1016/j.neuroimage.2009.09.007
 29. Egerton A, Brugger S, Raffin M, et al. Anterior cingulate glutamate levels related to clinical status following treatment in first-episode schizophrenia. *Neuropsychopharmacology*. 2012;37(11):2515-2521. doi:10.1038/npp.2012.113
 30. Boly M, Coleman MR, Davis MH, et al. When thoughts become action : An fMRI paradigm to study volitional brain activity in non-communicative brain injured patients. *Neuroimage*. 2007;36:979-992. doi:10.1016/j.neuroimage.2007.02.047
 31. Yoo S-S, Fairney T, Chen N, et al. Brain-computer interface using fMRI: spatial navigation by thoughts. *Neuroreport*. 2004;15(10):1591-1595.
doi:10.1097/01.wnr.0000133296.39160.fe
 32. Wong D, Schranz AL, Bartha R. Optimized in vivo brain glutamate measurement using long-echo-time semi-LASER at 7T. *NMR Biomed*. 2018:1-13.
doi:10.1002/nbm.4002
 33. First M, Williams J, Karg R, Spitzer R. Structured Clinical Interview for DSM-5 - Research Version (SCID-5 for DSM-5, Research Version; SCID-5-RV). *Am Psychiatr Assoc*. 2015.
 34. Peters SK, Dunlop K, Downar J. Cortico-striatal-thalamic loop circuits of the salience network: a central pathway in psychiatric disease and treatment. *Front*

Syst Neurosci. 2016;10:104. doi:10.3389/fnsys.2016.00104

35. Peirce J. PsychoPy - psychophysics software in Python. *J Neurosci Methods.* 2007;162(1-2):8-13.
36. Near J, Edden R, Evans CJ, Paquin R, Harris A, Jezzard P. Frequency and Phase Drift Correction of Magnetic Resonance Spectroscopy Data by Spectral Registration in the Time Domain. *Magn Reson Med.* 2015;73(1):44-50. doi:10.1002/mrm.25094.Frequency
37. Bartha R, Drost DJ, Menon RS, Williamson PC. Spectroscopic Lineshape Correction by QUECC: Combined QUALITY Deconvolution and Eddy Current Correction. *Magn Reson Med.* 2000;44:641-645.
38. Bartha R, Drost DJ, Williamson PC. Factors affecting the quantification of short echo in-vivo 1 H MR spectra: prior knowledge , peak elimination , and filtering. *NMR Biomed.* 1999;12:205-216.
39. IBM C. Released 2016. IBM SPSS Statistics for Windows, Version 24.0. Armonk, NY::IBM Corp.
40. Kumar J, Liddle EB, Fernandes CC, et al. Glutathione and glutamate in schizophrenia: a 7T MRS study. *Mol Psychiatry.* 2018. doi:10.1038/s41380-018-0104-7
41. Stanley JA, Raz N. Functional Magnetic Resonance Spectroscopy: The “New” MRS for Cognitive Neuroscience and Psychiatry Research. *Front Psychiatry.* 2018;9:1-12. doi:10.3389/fpsy.2018.00076

Chapter 4

4 Conclusion

In this thesis, we aimed to optimize our functional magnetic resonance spectroscopy protocol for detecting glutamate dynamics in response to a functional task, and to apply this in a group of never medicated first-episode schizophrenia expecting to reveal abnormal regulation of glutamate and glutathione compared to patient-matched group of healthy controls. Contrary to beliefs that the shortest possible echo time is best for metabolite observation using magnetic resonance spectroscopy, a longer echo time, when optimized, was found to better highlight the rephasing of signals from specific metabolites of interest and can be used in a functional MRS setting to detect metabolite dynamics in response to a functional paradigm. We also found that dynamic MRS measurements were more appropriate than traditional MRS measurements to reveal modulation of metabolite levels related to performance of a cognitive activation paradigm. Dynamic MRS, or fMRS, revealed better controlled differences of glutamate and glutathione regulation in both resting and active conditions when comparing first-episode schizophrenia to matched healthy controls. Our finding of prolonged elevation of GSH suggest that the human brain may have protective preparation response to potential near-future stimulation or oxidative stress based on administered cognitive stimulation.

4.1 Limitations

Though this work presented findings from glutathione dynamics along with glutamate dynamics, our specific fMRS sequence and echo time for clinical study (Chapter 3) was optimized for glutamate. Future approaches investigating glutathione, or other related metabolites such as glutamine and GABA, warrant methods optimized for those specific metabolites. Perhaps this limitation can lead to work on finding optimized approaches for best detection of multiple metabolites. Secondly, our current MRS measurements cannot distinguish between glutamate in the synaptic cleft, which is where glutamate

abnormalities related to schizophrenia are hypothesized to exist, and glutamate in the extracellular fluid^{1,2}. Though our functional paradigm alleviates this limitation slightly by focusing on glutamate regulation, in what we believe is occurring at the level of the synaptic cleft, instead of resting measurement of glutamate in the entire voxel, our tools cannot verify precisely that any glutamate abnormalities observed is purely a result of abnormalities in the synaptic cleft. Thirdly, our studies measured glutamate from only one part of the brain (dACC) without any other control region. We also were not able to include another related illness, such as major depressive disorder (MDD), to verify that any abnormalities observed in the dACC were specific to schizophrenia in the dACC (as was done in Taylor *et al.* 2015³). Lastly, our current MRS and fMRS analyses are made on a group-level. Increasing spectral resolution and optimizing metabolite signal detection are necessary improvements to translate this work from group-level analyses to individual-level analyses, a tool that would prove valuable for personally targeted care for patients with schizophrenia.

4.2 Future Works

Future direction of this work will include a longitudinal analysis of fMRS data based on our FES volunteer population at 6-month, 18-month, and 30-month follow-up appointments. Treatment outcome measures and symptom response assessments will be used to retrospectively evaluate the predictive power of the early scan data (0-month, never-medicated) to discriminate responders from non-responders. Another exciting avenue of research is the use of glutamate chemical exchange saturation transfer (GluCEST) as another tool to observe whole brain glutamate levels. This GluCEST protocol is under development, but once ready, is expected to provide higher metabolite signals as well as a whole brain perspective of glutamate behavior in response to cognitive activation.


It is important to continue glutamate and glutathione research in schizophrenia as early markers for stratifying responders and non-responders could have a disruptive effect on the current standard of care, especially for patients in the non-responder group. Empirical

evidence for sub-groups of schizophrenia patients experiencing different pathophysiological presentations of schizophrenia⁴ will help change the face of antipsychotic treatment to a better targeted treatment for each individual and will help untangle results and simplify the interpretation of drug trials for glutamate-based treatment approaches⁵.

4.3 References

1. Mark LP, Prost RW, Ulmer JL, Smith MM, Daniels DL, Strottmann JM, Brown WD, Hacin-Bey L. Pictorial Review of Glutamate Excitotoxicity: Fundamental Concepts for Neuroimaging. *Am J Neuroradiology*. 2001;22(10):1813-1824.
2. Hertz L, Yu ACH, Kala G, Schousboe A. Neuronal-astrocytic and cytosolic-mitochondrial metabolite trafficking during brain activation, hyperammonemia and energy deprivation. *Neurochem Int*. 2000;37(2-3):83-102.
3. Taylor R, Neufeld RWJ, Schaefer B, et al. Functional magnetic resonance spectroscopy of glutamate in schizophrenia and major depressive disorder: anterior cingulate activity during a color-word Stroop task. *npj Schizophr*. 2015;1:15028. doi:10.1038/npjSchz.2015.28
4. Howes OD, Kapur S. A neurobiological hypothesis for the classification of schizophrenia: type A (hyperdopaminergic) and type B (normodopaminergic). *Br J Psychiatry*. 2014;205:1-3. doi:10.1192/bjp.bp.113.138578
5. Stone JM. Glutamatergic antipsychotic drugs: a new dawn in the treatment of schizophrenia?. *Ther Adv Psychopharmacol*. 2011;1(1):5-18. doi:10.1177/2045125311400779

Appendix A: Ethics Approval



Research Ethics

**Western University Health Science Research Ethics Board
HSREB Amendment Approval Notice**

Principal Investigator: Dr. Lena Palaniyappan
Department & Institution: Schulich School of Medicine and Dentistry/Psychiatry, Western University

Review Type: Delegated
HSREB File Number: 108268
Study Title: The Pathophysiology of Thought Disorder in Psychosis (TOPSY)
Sponsor:

HSREB Amendment Approval Date: January 06, 2017
HSREB Expiry Date: October 24, 2017

Documents Approved and/or Received for Information:

Document Name	Comments	Version Date
Recruitment Items		2016/12/13
Instruments	Questionnaire	2016/11/23
Letter of Information & Consent	Patient LOI	2016/10/24
Revised Western University Protocol	Received 11/25/2016	
Letter of Information & Consent	Control LOI	2016/10/24


The Western University Health Science Research Ethics Board (HSREB) has reviewed and approved the amendment to the above named study, as of the HSREB Initial Approval Date noted above.

HSREB approval for this study remains valid until the HSREB Expiry Date noted above, conditional to timely submission and acceptance of HSREB Continuing Ethics Review.

The Western University HSREB operates in compliance with the Tri-Council Policy Statement Ethical Conduct for Research Involving Humans (TCPS2), the International Conference on Harmonization of Technical Requirements for Registration of Pharmaceuticals for Human Use Guideline for Good Clinical Practice Practices (ICH E6 R1), the Ontario Personal Health Information Protection Act (PHIPA, 2004), Part 4 of the Natural Health Product Regulations, Health Canada Medical Device Regulations and Part C, Division 5, of the Food and Drug Regulations of Health Canada.

Members of the HSREB who are named as Investigators in research studies do not participate in discussions related to, nor vote on such studies when they are presented to the REB.

The HSREB is registered with the U.S. Department of Health & Human Services under the IRB registration number IRB 00000940.


 Ethics Officer, on behalf of Dr. Joseph Gilbert, HSREB Chair

Ethics Officer: Urika Beale / Oshaya Harris / Nicole Kazuki / Grace Kelly / Vikki Tran / Karen Gopaul

Western University, Research, Support Services Bldg., Rm. 3150
 London, ON, Canada N6G 1G9 t. 519.861.3036 f. 519.850.2466 www.uwo.ca/research/ethics

Appendix A Ethics approval

Appendix B: Supplementary Figures

Group	$p(\text{Stroop-Rest})$	$p(\text{Rec1-Stroop})$	$p(\text{Rec1-Rec2})$	Rest	Stroop	Recovery1	Recovery2
<i>TE=60ms</i>							
Glu/NAA	0.549	0.551	0.670	0.70 ±0.02	0.71 ±0.02	0.70 ±0.02	0.71 ±0.02
Glu/Cr	0.601	0.372	0.472	1.03 ±0.03	1.04±0.03	1.02±0.03	1.03±0.02
GSH/NAA	0.022	0.208	0.629	0.36 ±0.01	0.33 ±0.01	0.35 ±0.02	0.35 ±0.01
GSH/Cr	0.043	0.324	0.389	0.52 ±0.02	0.49 ±0.02	0.51 ±0.02	0.52 ±0.02
<i>TE=100ms</i>							
Glu/NAA	0.468	0.688	0.153	0.63 ±0.01	0.63 ±0.01	0.64 ±0.01	0.62 ±0.01
Glu/Cr	1.000	0.873	0.006	0.86 ±0.02	0.85 ±0.02	0.85 ±0.02	0.82 ±0.02
GSH/NAA	0.430	0.134	0.325	0.19 ±0.01	0.20 ±0.01	0.22 ±0.01	0.21 ±0.01
GSH/Cr	0.440	0.284	0.357	0.26 ±0.01	0.28 ±0.01	0.29 ±0.01	0.28 ±0.01

Appendix B-1. Pairwise comparison of mean glutamate and glutathione signal ratios (relative to NAA and Cr), with standard error of means, for TE=60ms (N=12) and TE=100ms (N=12). Statistically significant values are bolded.

Group	$p(\text{Stroop-Rest})$	$p(\text{Rec1-Stroop})$	$p(\text{Rec1-Rec2})$	Rest	Stroop	Recovery1	Recovery2
<i>HC</i>							
Glu/NAA	0.690	0.449	0.214	0.63 ±0.01	0.62 ±0.01	0.63 ±0.01	0.62 ±0.01
Glu/Cr	0.246	0.707	0.520	0.85 ±0.01	0.84 ±0.01	0.84 ±0.01	0.83 ±0.01
GSH/NAA	0.042	0.090	0.065	0.20±0.00	0.21±0.01	0.23±0.01	0.21±0.01
GSH/Cr	0.017	0.207	0.159	0.27±0.01	0.29±0.01	0.30±0.01	0.29±0.01
<i>FES</i>							
Glu/NAA	0.461	0.273	0.782	0.61 ±0.01	0.62 ±0.01	0.61 ±0.01	0.61 ±0.01
Glu/Cr	0.283	0.154	0.470	0.82 ±0.02	0.83 ±0.02	0.82 ±0.02	0.81 ±0.02
GSH/NAA	0.504	0.609	0.882	0.22±0.01	0.21±0.01	0.21±0.01	0.21±0.01
GSH/Cr	0.508	0.574	0.953	0.29±0.01	0.28±0.01	0.28±0.01	0.28±0.01

Appendix B-2. Pairwise comparison of mean glutamate and glutathione signal ratios (relative to NAA and Cr), with standard error of means, for HC (N=25) and FES (N=21). Statistically significant values are bolded.

<i>Group</i>	<i>Rest</i> [mM]	<i>Stroop</i> [mM]	<i>Recovery 1</i> [mM]	<i>Recovery 2</i> [mM]
<i>TE=60ms</i>				
Alanine	0.13±0.05	0.21±0.10	0.14±0.07	0.16±0.07
Aspartate	1.14±0.20	0.97±0.18	0.82±0.18	0.77±0.26
Choline	2.43±0.07	2.47±0.07	2.43±0.08	2.43±0.07
Creatine	9.44±0.25	9.48±0.23	9.42±0.22	9.30±0.22
GABA	2.03±0.24	2.31±0.36	2.00±0.31	1.87±0.38
Glucose	2.09±0.12	2.12±0.12	2.03±0.09	2.10±0.13
Glutamate	9.31±0.44	9.53±0.46	9.25±0.40	9.34±0.38
Glutamine	0.31±0.15	0.25±0.13	0.29±0.14	0.40±0.19
Glutathione	2.79±0.12	2.64±0.14	2.73±0.12	2.77±0.10
Glycine	0.27±0.07	0.33±0.14	0.33±0.09	0.39±0.11
Lactate	0.09±0.05	0.21±0.08	0.24±0.07	0.14±0.09
Myo-inositol	5.79±0.14	5.91±0.16	5.74±0.10	5.84±0.18
N-Acetyl Aspartate	12.15±0.32	12.28±0.30	12.15±0.31	12.06±0.33
N-Acetyl-Aspartyl Glutamate	0.28±0.08	0.21±0.07	0.26±0.09	0.34±0.11
Phosphorylethanolamine	15.73±0.98	14.18±1.13	13.31±1.63	13.86±1.00
Scyllo-inositol	0.21±0.02	0.23±0.03	0.22±0.02	0.22±0.03
Taurine	3.06±0.61	2.93±0.69	2.69±0.48	3.25±0.46
<i>TE=100ms</i>				
Alanine	0.17±0.06	0.17±0.04	0.19±0.05	0.15±0.04
Aspartate	0.00±0.00	0.00±0.00	0.00±0.00	0.00±0.00
Choline	2.39±0.09	2.39±0.09	2.39±0.09	2.35±0.10
Creatine	8.33±0.29	8.39±0.29	8.31±0.31	8.32±0.31
GABA	0.00±0.00	0.00±0.00	0.00±0.00	0.00±0.00
Glucose	0.42±0.10	0.38±0.10	0.36±0.09	0.40±0.09
Glutamate	6.52±0.31	6.47±0.32	6.64±0.37	6.35±0.33
Glutamine	0.98±0.09	1.05±0.11	1.00±0.08	1.05±0.11
Glutathione	1.51±0.07	1.61±0.06	1.64±0.08	1.63±0.08
Glycine	0.01±0.01	0.00±0.00	0.00±0.00	0.00±0.00
Lactate	0.06±0.02	0.08±0.02	0.13±0.03	0.09±0.03
Myo-inositol	4.69±0.21	4.71±0.23	4.67±0.23	4.55±0.22
N-Acetyl Aspartate	10.31±0.38	10.38±0.38	10.39±0.41	10.23±0.38
N-Acetyl-Aspartyl Glutamate	0.03±0.03	0.01±0.01	0.02±0.02	0.02±0.02
Phosphorylethanolamine	2.00±0.64	1.50±0.56	1.95±0.76	1.07±0.52
Scyllo-inositol	0.30±0.04	0.31±0.04	0.29±0.03	0.31±0.03
Taurine	1.22±0.15	0.98±0.15	1.24±0.13	1.03±0.12

Appendix B-3. Mean concentration, with standard error of means, of all quantifiable metabolites using fitting template for TE=60ms (N=12) and TE=100ms (N=12).

<i>Group</i>	<i>Rest</i> [mM]	<i>Stroop</i> [mM]	<i>Recovery 1</i> [mM]	<i>Recovery 2</i> [mM]
<i>HC</i>				
Alanine	0.14±0.03	0.18±0.03	0.20±0.03	0.19±0.03
Aspartate	0.00±0.00	0.00±0.00	0.00±0.00	0.00±0.00
Choline	2.47±0.06	2.46±0.06	2.46±0.06	2.37±0.06
Creatine	8.50±0.18	8.56±0.18	8.50±0.19	8.37±0.18
GABA	0.00±0.00	0.00±0.00	0.00±0.00	0.00±0.00
Glucose	0.43±0.07	0.43±0.07	0.50±0.09	0.44±0.07
Glutamate	6.61±0.19	6.63±0.20	6.60±0.20	6.46±0.20
Glutamine	1.07±0.06	1.06±0.06	1.03±0.05	1.06±0.06
Glutathione	1.48±0.05	1.61±0.04	1.67±0.06	1.58±0.04
Glycine	0.00±0.00	0.00±0.00	0.00±0.00	0.00±0.00
Lactate	0.08±0.02	0.11±0.01	0.10±0.02	0.11±0.02
Myo-inositol	4.67±0.14	4.75±0.14	4.83±0.15	4.62±0.13
N-Acetyl Aspartate	10.40±0.23	10.45±0.23	10.41±0.24	10.23±0.22
N-Acetyl-Aspartyl Glutamate	0.02±0.02	0.00±0.00	0.01±0.01	0.03±0.02
Phosphorylethanolamine	3.40±0.61	2.12±0.51	2.62±0.58	1.90±0.53
Scyllo-inositol	0.27±0.02	0.29±0.02	0.30±0.02	0.30±0.02
Taurine	1.05±0.09	0.90±0.09	1.09±0.09	1.00±0.09
<i>FES</i>				
Alanine	0.18±0.04	0.21±0.03	0.15±0.04	0.22±0.03
Aspartate	0.00±0.00	0.00±0.00	0.00±0.00	0.00±0.00
Choline	2.58±0.11	2.60±0.12	2.58±0.12	2.54±0.12
Creatine	9.07±0.36	9.15±0.40	9.07±0.38	9.00±0.38
GABA	0.00±0.00	0.00±0.00	0.00±0.00	0.00±0.00
Glucose	0.46±0.08	0.45±0.09	0.43±0.09	0.44±0.07
Glutamate	6.81±0.27	6.95±0.29	6.77±0.30	6.67±0.27
Glutamine	1.12±0.07	1.10±0.07	1.06±0.09	1.16±0.08
Glutathione	1.74±0.08	1.69±0.06	1.65±0.07	1.65±0.08
Glycine	0.00±0.00	0.00±0.00	0.00±0.00	0.00±0.00
Lactate	0.11±0.02	0.13±0.02	0.13±0.02	0.15±0.02
Myo-inositol	4.82±0.24	4.95±0.24	4.81±0.23	4.54±0.32
N-Acetyl Aspartate	10.99±0.38	11.11±0.41	10.95±0.40	10.92±0.40
N-Acetyl-Aspartyl Glutamate	0.03±0.02	0.02±0.01	0.04±0.04	0.01±0.01
Phosphorylethanolamine	2.51±0.88	2.52±0.69	3.07±0.85	2.13±0.52
Scyllo-inositol	0.34±0.03	0.32±0.03	0.34±0.02	0.34±0.03
Taurine	1.12±0.10	1.14±0.11	1.09±0.12	1.16±0.09

Appendix B-4. Mean concentration, with standard error of means, of all quantifiable metabolites using fitting template for HC (N=25) and FES (N=21).

Appendix B Supplementary tables and figures

Curriculum Vitae

Name: Peter Jeon

Post-secondary Education and Degrees:

Department of Medical Biophysics
The University of Western Ontario
London, Ontario, Canada
2016-2019 M.Sc.

Specialization in Medical Physics (Honors)
The University of Western Ontario
London, Ontario, Canada
2012-2016 B.Sc.

Specialization in Biology (Honors)
University of Western Ontario
London, Ontario, Canada
2007-2012 B.Sc.

Related Work Experience:

Teaching Assistant (Supervisor: Dr. Chris Ellis)
Medical Biophysics 3507G: *Analysis of Oxygen Transport in Biological Systems*
The University of Western Ontario
Jan. 2018 - April 2018

Teaching Assistant (Supervisor: Dr. Neil Gelman)
Medical Biophysics 3505F: *Mathematical Transform Applications in Medical Biophysics*
The University of Western Ontario
Sept. 2017 - Dec. 2017

Summer Research Assistant (Supervisors: Dr. Jean Théberge & Lena Palaniyappan)
Dynamic glutamate abnormalities in schizophrenia and major depressive disorder
The University of Western Ontario
June 2016 - August 2016

Undergraduate Research Student (Supervisor: Dr. Charles McKenzie)
Visceral and subcutaneous fat quantification using MATLAB
The University of Western Ontario
Jan. 2013 - Mar. 2014

- Oral Presentations:** Academic Research Day
“Measuring glutamate and glutathione dynamics in first-episode schizophrenia using 7.0-Tesla functional magnetic resonance spectroscopy”
 June 27, 2019
- Discovery Roberts Tour
“Human brain functional magnetic spectroscopy at 7-Tesla”
 February 15, 2018
- Neuroimaging in Mental Illnesses Seminar
“Detecting changes in human brain glutamate using 7-Tesla functional magnetic resonance spectroscopy”
 January 30, 2018
- UWO Medical Biophysics Department Seminar
“Detecting changes in human brain glutamate using 7-Tesla functional magnetic resonance spectroscopy at short versus long echo times”
 January 25, 2018
- London Imaging Discovery Day
“Dynamic glutamate functional magnetic resonance spectroscopy measurements in schizophrenia at 7-Tesla”
 June 27, 2017
- UWO Medical Biophysics Department Seminar
“Dynamic glutamate functional magnetic resonance spectroscopy and treatment response in schizophrenia”
 March 23, 2017
- CFMM Winter School Scholarship Program
“Dynamic glutamate functional magnetic resonance spectroscopy and treatment response in schizophrenia”
 March 17, 2017
- Poster Presentation:** Developmental Disabilities Research Day
“Brain metabolite dynamics in first-episode schizophrenia using 7.0-Tesla functional magnetic resonance spectroscopy”
 May 30, 2019
- Neuroscience Research Day
“Functional magnetic resonance spectroscopy in schizophrenia: A 7.0-Tesla study”
 May 10, 2019

Joint London Mental Health Research Day
“Functional glutamate measurements in first-episode schizophrenia using 7-Tesla magnetic resonance spectroscopy”
June 14, 2018

London Health Research Day
“Echo time comparison for detecting human brain glutamate changes using 7-Tesla functional magnetic resonance”
spectroscopy”
May 10, 2018

Awards:

Western Graduate Research Scholarship (WGRS)
\$1500 (CDN)/term
Sept. 2017 - Apr.2018

CFMM Winter School Scholarship Program
All expenses covered
Mar. 2017

Western Graduate Research Scholarship (WGRS)
\$1500 (CDN)/term
Sept. 2016 - Apr.2017

The Western Scholarship of Excellence
\$2000 (CDN)
Sept. 2007 - Apr.2008